ROYAL SOCIETY
OF CHEMISTRY

REVIEW

Check for updates

Supramolecular agents for combination of photodynamic therapy and other treatments

Nahyun Kwon, [ID] b Heejeong Kim, [ID] b Xingshu Li [ID] *a and Juyoung Yoon [ID] *b

Photodynamic therapy (PDT) is a promising treatment for cancers such as superficial skin cancers, esophageal cancer, and cervical cancer. Unfortunately, PDT often does not have sufficient therapeutic benefits due to its intrinsic oxygen dependence and the limited permeability of irradiating light. Side effects from "always on" photosensitizers (PSs) can be problematic, and PDT cannot treat tumor metastases or recurrences. In recent years, supramolecular approaches using non-covalent interactions have attracted attention due to their potential in PS development. A supramolecular PS assembly could be built to maximize photodynamic effects and minimize side effects. A combination of two or more therapies can effectively address shortcomings while maximizing the benefits of each treatment regimen. Using the supramolecular assembly, it is possible to design a multifunctional supramolecular PS to exert synergistic effects by combining PDT with other treatment methods. This review provides a summary of important research progress on supramolecular systems that can be used to combine PDT with photothermal therapy, chemotherapy, and immunotherapy to compensate for the shortcomings of PDT, and it provides an overview of the prospects for future cancer treatment advances and clinical applications.
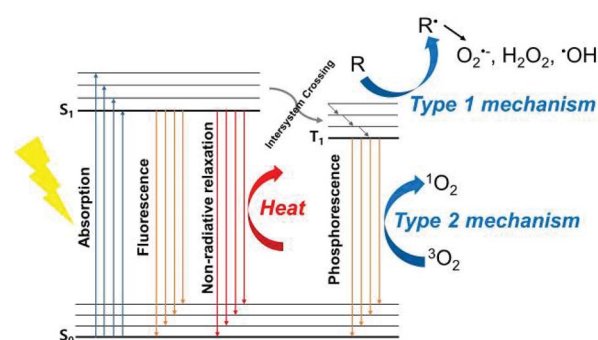
1. Introduction

1.1 Brief introduction to PDT

1.1.1 Photophysical and photochemical mechanisms of PDT. Photodynamic therapy (PDT) is a process by which a photosensitizer (PS) activated by light releases energy in a way that produces cytotoxicity. When a PS is activated by visible or near-infrared (NIR) light in the wavelength range of 400–900 nm, it is transformed from the ground singlet state (S_0) to the excited singlet state (S_1) (Scheme 1).[1] To return from the S_1 state back to the stable S_0, it can generate heat using non-radioactive decay pathways, or it can emit radiation as fluorescence. Because the S_1 state has a very short lifetime (in nanosecond units), it reaches the excited triplet state, which has a relatively long lifetime, through intersystem crossing (ISC). Depending on the photochemical reaction that occurs when energy is released from the triplet state, PDT progression is classified into two paths.[2] The first is a type I mechanism, which generates a superoxide anion radical ($O_2^{\cdot-}$), hydrogen peroxide (H_2O_2), and hydroxyl radicals ($HO^{\cdot}$) by transferring electrons to the adjacent substrates. The type II mechanism transfers energy directly to molecular oxygen (O_2) to produce a singlet oxygen

($^1O_2$). Most PSs follow the type II mechanism, which is why most photodynamic reactions are oxygen dependent.[3] The type I and type II mechanisms can also occur simultaneously, and the structural characteristics of a PS and its environment can affect which mechanism dominates the reaction.

1.1.2 PDT-mediated cytotoxicity. When tumor cells absorb a PS, it is localized in several organelles (the mitochondria, lysosomes, endoplasmic reticulum, plasma membrane, *etc.*), and then it produces highly cytotoxic reactive oxygen species (ROS) through the PDT process. The extremely short-lived ROS cause cell damage only within a 10–55 nm range around the PS.[4] Apoptosis is the major mode of cell death that is commonly caused by PDT.[5] The mechanism that causes necrosis is not yet

College of Chemistry, State Key Laboratory of Photocatalysis on Energy and Environment, Fujian Provincial Key Laboratory of Cancer Metastasis Chemoprevention and Chemotherapy, Fuzhou University, Fuzhou 350116, China. E-mail: xingshuli@fzu.edu.cn

Department of Chemistry and Nanoscience, Ewha Womans University, Seoul 03760, Korea. E-mail: jyoon@ewha.ac.kr

Scheme 1 Modified Jablonski diagram of the photophysical processes involved in PDT.

fully understood, but severe mitochondrial membrane damage can cause necrosis.[6] The autophagy pathway breaks down organelles using lysosomes and can be triggered by oxidative stress signals from ROS.[7] Damage to organelles caused by the photodynamic reaction of the localized PS can directly kill tumor cells through apoptosis and non-apoptotic (necrotic, and autophagy) pathways.[8] PDT also affects tumor microvessels, closing blood vessels and thereby blocking the delivery of oxygen and nutrients, causing severe tissue hypoxia.[9,10] These effects upregulate the expression of the vascular endothelial growth factor and cyclooxygenase in tumor tissue after PDT.[11,12] When cells and vascular systems are stressed by PDT, a local inflammatory response is triggered, releasing cytokines and stress-responsive proteins,[13] which can induce a variety of immune responses, such as an influx of leukocytes, which are involved in tumor removal activities.[14]

1.1.3 History of clinical applications of PDT. Light has been used to treat diseases since the ancient civilizations of Egypt, China, Greece, India, and Rome.[15] Despite its long history, the first literature to report the concept of PDT using light-responsive dyes was the work of Oscar Raab in the 1900s. He observed that acridine orange that accumulated in Paramesia showed cytotoxicity after exposure to light.[16] His supervisor, Hermann von Tappeiner, confirmed that atmospheric oxygen plays an important role in this toxicity and defined this reaction as a 'photodynamic action'.[17] The discovery of hematoporphyrin (HP) was a very important event in the history of PDT. In 1961, Lipson discovered that a mixture of hematoporphyrin derivatives (HpDs) obtained after acid treatment with HP emitted tumor-localized fluorescence.[18] After that, HpD mixtures were found to have therapeutic effects under incandescent light irradiation.[19] The clinical application of PDT as we know it today is due to efforts led by Dougherty in the 1970s.

After his work in 1975 on treating tumors in mice with HpD,[20] he treated various patients with tumors and confirmed the therapeutic effects of HpD.[21,22] The exact composition of HpDs has still not been determined, though it is a compound of various porphyrins. However, the main active ingredient is dihematoporphyrin ether (DHE) that is produced when hematoporphyrin is converted to HpD by acetylation. The work establishing the activity of DHE led to the development of a more purified and better-characterized version of HpD, Photofrin®, which was first approved by Canadian regulatory authorities for the treatment of bladder cancer. Photofrin® was approved by the U.S. Food and Drug Administration (FDA) in 1995 as a PS for the treatment of esophageal cancer.[23,24] This substance is still the PS most frequently approved for clinical use. Since the approval of Photofrin®, the first-generation PS, many new PSs have been developed and approved.[25,26] Second-generation PSs, such as 5-aminolevulinic acid (ALA) derivatives and chlorin derivatives, generally have a longer absorption wavelength than the first-generation PS. ALA, a porphyrin precursor, was approved by the FDA in 1999 under the name Levulan® for the treatment of actinic keratoses. Foscan®, a chlorin derivative, was approved in Europe in 2001 for the treatment of a variety of tumors. In addition, several candidates, such as phthalocyanine derivatives and texaphyrin derivatives, are in clinical trials as PSs for tumor treatment (Table 1).[8]

1.1.4 Development of photosensitizers. In addition to classical PSs that have been approved or are in clinical trials, studies are being conducted to develop new, more effective PSs. An ideal PS should have a long wavelength with a deep transmission depth as its maximum absorption wavelength, and the ISC efficiency between the excited singlet state and the triplet state must be high. To date, the potential of many organic and inorganic substances as PSs has been explored.[27]

Table 1 Clinically applied photosensitizers. Adapted with permission from ref. 8. Copyright 2011 American Cancer Society, Inc[a]

Photosensitizer	Structure	Wavelength (nm)	Approved	Trials	Cancer types
Porfimer sodium (Photofrin) (HpD)	Porphyrin	630	Worldwide		Lung, esophagus, bile duct, bladder, brain, ovarian
ALA	Porphyrin precursor	635	Worldwide		Skin, bladder, brain, esophagus
ALA esters	Porphyrin precursor	635	Europe		Skin, bladder
Temoporfin (Foscan) (mTHPC)	Chlorine	652	Europe	United States	Head and neck, lung, brain, skin, bile duct
Verteporfin	Chlorine	690	Worldwide (AMD)	United Kingdom	Ophthalmic, pancreatic, skin
HPPH	Chlorin	665		United States	Head and neck, esophagus, lung
SnEt2 (Purlytin)	Chlorin	660		United States	Skin, breast
Talaporfin (LS11, MACE, NPe6)	Chlorin	660		United States	Liver, colon, brain
Ce6-PVP (Fotolon), Ce6 derivatives (Radachlorin, Photodithazine)	Chlorin	660		Belarus, Russia	Nasopharyngeal, sarcoma, brain
Silicon phthalocyanine (Pc4)	Phthalocyanine	675		United States	Cutaneous T-cell lymphoma
Padoporfin (TOOKAD)	Bacteriochlorin	762		United States	Prostate
Motexafin lutetium (Lutex)	Texaphyrin	732		United States	Breast

[a] Abbreviations: ALA, 5-aminolevulinic acid; AMD, age-related macular degeneration; Ce6-PVP, chlorin e6-polyvinypyrrolidone; HPD, hematoporphyrin derivative; HPPH, 2-(1-hexyloxyethyl)-2-devinyl pyropheophorbide-a; MACE, mono-(L)-aspartylchlorin-e6; mTHPC, m-tetrahydroxyphenylchlorin; SnEt2, tin ethyl etiopurpurin.

Organic PSs have relatively high biocompatibility, which is advantageous in clinical trials. Because precise molecular design and modification are possible, it is easy to introduce characterization groups, so it is easy to modify them to have better therapeutic effects. First-generation organic PSs include porphyrin derivatives, such as the aforementioned HpD. However, it has a short excitation wavelength, low tumor selectivity, and long-term accumulation in normal tissues and the skin, causing light sensitivity.[28] Second-generation PSs, such as porphyrin derivatives and chlorin derivatives, have a clear composition and are excited at longer wavelengths to take advantage of light that penetrates deeper into tissue.[29] In addition to classic dyes with a tetrapyrrole structure, various synthetic dyes are being tested for use as PSs. A variety of cyanine dyes can be used in PDT.[30,31] Indocyanine green (ICG) is a water-soluble, anionic, tricarbocyanine dye approved by the FDA. ICG has the property of generating heat and ROS upon NIR irradiation.[32,33] Methylene blue is a widely used dye that is also used to treat basal cell carcinoma, melanoma, and fungal infections.[34] Rose bengal, which has a long history as a photoactive dye, has also been studied for anticancer applications.[35] BODIPY dye can function as a PS if a halogen atom is added or an electron donating group is introduced to increase the triplet yield.[36–39] In addition, squaraine dyes and transition metal compounds such as ruthenium(II) polypyridyl complexes are being studied as PSs.[40,41]

Inorganic PSs usually have stronger light absorption and higher light stability than organic PSs. Photocatalysts such as titanium dioxide (TiO_2), semiconductors (CdSe, ZnO, *etc.*), and Ag, Pt, and Au nanoparticles have been used as inorganic PSs.[42–46] Unlike most of the organic PSs, which have a high dependence on the type II PDT process, some inorganic PSs can produce radicals or radical ions without oxygen dependence *via* the type I photoreaction mechanism, giving them a high value in treating hypoxic tumors.[47] However, inorganic PSs have the fatal disadvantage of low biocompatibility, so many issues must be addressed before clinical applications will be feasible.

The main topic in the development of third-generation PSs is delivery systems. The use of nanosystem is an approach to improve the water solubility of existing PSs and increase delivery efficiency.[48–50] Researchers have tried various methods to use the aforementioned TiO_2 and ZnO inorganic nanoparticles as photodynamic therapeutics.[44] Metallic nanoparticles such as gold nanoparticles can exhibit photothermal therapy (PTT) effects and can be used as carriers for PSs.[51] Micelles or liposomes made from biodegradable polymers can be effective nanosystems that have high biocompatibility and plasma circulation times.[50] Nanoparticles are endowed with passive targeting ability, *i.e.*, they accumulate intensively in tumor tissue through enhanced permeability and retention (EPR) effects.[52–54] In addition, active targeting strategies that use a targeting ligand or a tumor microenvironment reactive group on the surface of a nanocarrier can further improve tumor selectivity.[55,56]

1.1.5 Limitations of PDT. Compared with traditional treatments such as surgery, chemotherapy, and radiation therapy, PDT offers several advantages. As a non-invasive method, PDT can be used for end-stage cancer patients with reduced stamina because it carries a low risk of bleeding or complications. In addition, it is easy to change the light irradiation site, time, and power, allowing precise control of treatment. Nonetheless, significant drawbacks limit the clinical application of PDT. First, treatment of deep tumors is difficult due to the shallow depth of light transmission through biological tissues.[57] Second, the PDT process, especially the type II pathway, is oxygen-dependent, which greatly hinders the therapeutic effect in hypoxic tumor microenvironments.[58] Third, residual PSs remaining in the skin or other normal tissues can make patients sensitive to light, producing a risk of side effects.[59] Finally, because most PSs are highly conjugated hydrophobic molecules, they aggregate strongly in aqueous solutions. PS aggregation generally quenches photodynamic activity, thereby interfering with PS operation *in vivo*. To expand the successful clinical applications of PDT, future PS development must improve these shortcomings.

1.2 Combination treatment with PDT

It is difficult to completely eradicate solid tumors using PDT treatment alone because of the inherent limitations just discussed. Even if delivery and selectivity are improved, PDT is activated by light irradiation, so it is difficult to treat deep tissues or metastatic tumors out of the reach of light. Therefore, PDT is generally combined with other types of treatments to complement the shortcomings and maximize the strengths of each treatment and ideally produce synergistic effects.[60]

PTT is not oxygen dependent, so it can complement PDT that uses oxygen to generate ROS. In addition, the increase in the local temperature caused by PTT promotes blood flow, improves drug delivery efficiency, and can alleviate hypoxia in tumor tissue. Supramolecular PSs function not only as therapeutic agents, but also as carriers, and can thus increase the efficiency of delivering hydrophobic anticancer drugs to the tumor site. A combination of phototherapy and chemotherapy reduces the likelihood of tumor recurrence after PDT. Immunotherapy, the most popular cancer treatment therapy in recent years, can offer synergistic effects with PDT. Tumor cells that are killed by light therapy have been shown to amplify the antitumor immune response by triggering the release of immune-inducing substances, thereby overcoming the low immune response rate that is the biggest obstacle to clinical applications of cancer immunotherapy.

1.3 Supramolecular approach to constructing nanophotosensitizers

With the development of nanotechnology, supramolecular self-assembled PSs that use non-covalent interactions are drawing attention as innovative nanomaterials.[61] Supramolecular chemistry combines two or more molecules with non-covalent forces such as electrostatic interactions (ions, hydrogen bonding, and halogen bonding), π–π interactions, host–guest interactions, hydrogen bonding, and metal coordination. In particular, intermolecular interactions with PS molecules caused by supramolecular self-assembly can affect ROS

production.[62] The internal conversion rate and contact quenching, which change depending on the intermolecular distance, can control fluorescence emissions and PDT and PTT efficiency. Controlling the ROS decrease or increase in cells is important because it can be used to control PSs that are present in an "always on" state to reduce side effects or produce enhanced PDT effects. For this reason, the application of supramolecular self-assembled nanoparticles to PDT therapy has been accelerating in recent years.[63] An even more attractive feature of supramolecular chemistry is that it can break the subtle balance maintained by assembled nanosystems using small changes in pH, and temperature, or a trigger in the surrounding environment.[64] This property can be used to design activatable nanoassemblies specific to the tumor microenvironment.

1.3.1 Reduction of ROS production by supramolecular formation.
Direct contact between molecules can produce strong quenching of fluorescence and ROS generation. This is attractive because it can be used as a control strategy to prevent unwanted photodynamic activation from occurring before the PS reaches the target tissue. If supramolecular assembly PSs are designed to react to triggers that dissolve aggregation, they can be switchable. Inducing an appropriate supramolecular assembly is an efficient approach to induce desirable photophysical changes without causing chemical changes. Xing *et al.* reported a co-assembly strategy for GO, albumin, and a PS (chlorine e6, Ce6). The high level of aggregation caused by direct contact between the GO and Ce6 meant that the nanocomposites produced less ROS than free Ce6. However, the assembly underwent enzymatic degradation in intracellular lysosomes and then exhibited very high fluorescence intensity.[65] Liu *et al.* also reported a supramolecular PS that reduces ROS by using the self-quenching state of tannic acid and Ce6. Fluorescence quenching and a reduced ability to produce ROS were observed after cell internalization.[66] In addition, a supramolecular assembly can induce "supramolecular photothermal effects."[67] In a densely packed system, intrinsic fluorescence is severely dissipated by increased internal conversion (*i.e.*, a nonradiative process), and the remaining energy is converted into heat. This mechanism is similar to the aggregation caused quenching (ACQ) effect and can significantly improve the photothermal conversion efficiency of supramolecular assemblies. Recently, the Yoon group observed fully quenched fluorescence and reduced $^1O_2$ production following the direct self-assembly of two water-soluble phthalocyanine derivatives. These experiments produced nanoassemblies with high photoacoustic and photothermal activity.[68]

1.3.2 Increasing ROS production through supramolecular formation.
Enhancing the ISC efficiency can increase ROS generation. Several recently published studies have reported that coordinating certain metals or introducing heavy atoms can increase the ROS production of PSs.[69,70] Guo *et al.* introduced platinum (Pt) to increase the intersystem efficiency of the BODIPY fluorophore, and found that nanoparticles composed of Pt-BODIPY showed improved $^1O_2$ production ability.[71] Aggregation generally induces self-quenching, but supramolecular approaches of molecules that are bulky and space-consuming can prevent self-quenching by aggregation. In such systems, fluorescence emissions and photophysical processes such as ISC can be improved on a principle similar to the aggregation-induced emission (AIE) effect.[72] The Liu group applied nanoparticles from materials with AIE properties to PDT.[73,74] Adjusting the distance between aggregated compounds can also control the photothermal conversion performance. In a study carried out by the Tang group, chromophores kept far apart by a 2-decyl myristyl group maintained high photothermal efficiency.[75] The energetic stabilization of the twisted intramolecular charge transfer state increases photothermal properties by ACQ. On the other hand, closely aggregated chromophores inhibit intramolecular motion and charge transfer, resulting in the emission of less light and heat.

1.3.3 Photophysical changes by supramolecular assembly.
Supramolecular assembly can cause red or blue absorption shifts by means of J-type or H-type aggregation.[76] The J aggregates involved in shifting absorption toward long wavelengths are attracting particular scientific attention because they could enable the development of a PS capable of absorbing a wavelength long enough to be suitable for bio-applications. For example, the BODIPY derivative compound reported by He *et al.* exhibits an absorption peak with a red shift of about 100 nm in the supramolecular assembly form compared with the monomer form.[77] This suggests the formation of J-shaped aggregates of BODIPY molecules. Cheng *et al.* reported that aza-BODIPY-lipid building blocks self-assemble into liposomal nanoparticles *via* J-aggregation. These particles have an absorption wavelength in the NIR region and photoacoustic properties.[78]

1.3.4 Increasing light stability through supramolecular assembly.
Supramolecular encapsulation can also be a photostabilizing strategy. Self-assembled molecular capsules such as cyclodextrins, cucurbit[7]urils, and rotaxanes increase the photostability of fluorescent dyes.[79,80] Supramolecular assembly preserves the photophysical and photochemical properties of chemically unstable species by reducing the chance that monomer molecules will come into contact with the external environment or solvent.

1.4 Supramolecular approach to multimodal therapy

This review article summarizes the use of supramolecular assemblies to make nanostructured PSs. The supramolecular approach can improve the photophysical efficiency of PSs, and supramolecular assemblies such as micelles and liposomes can be used to carry drugs. Synergistic interactions between PDT and other treatments that can be achieved through simple supramolecular assemblies can produce a much stronger anticancer effect than either treatment alone, along with providing high stability, photoactivity, and tumor targeting ability.

2. Supramolecular agents to combine PDT and PTT

PTT is another non-invasive phototherapy strategy that uses PSs. Unlike PDT, which has to generate ROS to kill cancer cells, photothermal agents excited by light release energy as heat

through non-radiative decay. Localized overheating caused by PTT damages the surrounding cell membranes or causes protein denaturation. In addition to killing cancer cells, photothermal agents offer the possibility of photoacoustic (PA) imaging. PA imaging is the transformation of sound waves generated by thermal expansion due to the PTT effect into visual signals. The generated sound waves enable imaging of deep tissues with minimal signal loss.

The most frequently studied photothermal materials are nanoparticles of precious metals such as Au, Ag, and Pt.[81] Although they have high photothermal conversion efficiency, they are expensive and have low biodegradability, making them largely inappropriate for biomedical applications. Carbon materials such as graphene and carbon nanosheets have also been studied, but their NIR absorption capacity is poor.[82] Recently, metallic–nonmetallic compounds such as CuS and organic semiconducting nanomaterials have been developed as photothermal agents.[83] Organic nanomaterials can solve the non-biocompatibility problem of inorganic photothermal materials, but their low photothermal conversion efficiency and complex manufacturing processes remain limitations.[84]

The difference between PDT and PTT is that PTT does not depend on the oxygen concentration. Therefore, when they are used in combination, PTT can complement the oxygen dependence of PDT. In addition, the heat generated by PTT can increase blood flow within the tumor to promote PS delivery to the cells and enrich the tumor oxygen levels, increasing PDT efficiency. Furthermore, multimodal imaging can use both the fluorescence signal of the PDT and the PA signal caused by the photothermal effect. Wang et al. connected Ce6 to a gold nanorod surface using an aptamer switch probe.[85] The conjugated PS provided a significantly improved therapeutic effect compared with PDT or PTT treatment alone. Liu et al. achieved good PTT/PDT synergies by loading ICG molecules onto upconversion nanoparticles.[86]

Another notable fact about combining PDT and PTT is that self-assembly of PSs for PDT often induces supramolecular photothermal effects.[87] For example, Lovell et al. self-assembled a lipid-mimicking molecule containing pyropheophorbide-a into nanovesicles called "porphysomes."[88] These vesicles were capable of fluorescence quenching, PA imaging, and PTT, and they showed an activatable fluorescence signal upon tumor accumulation. Tumor-bearing mice showed complete tumor remission and 100% survival 28 days after porphysome administration and laser treatment. Furthermore, porphysomes can be loaded with chemotherapeutic agents and radiolabeled, making them a very promising therapeutic molecule. The porphyrin–peptide assembled nano-dots reported by Zou et al. achieved high-efficiency photothermal energy conversion by completely quenching fluorescence and inhibiting the generation of ROS with strong π-stacking.[89] Consisting of a single component, this material acquired photothermal and PA properties through self-assembly. In the sections that follow, we introduce a variety of methods for engineering synergistic photodynamic and photothermal nanosystems using supramolecular assembly.

2.1 Single-component supramolecule—supramolecular photothermal effects

The photothermal effects induced by supramolecular assembly make possible an activatable supramolecular nano-photosensitive agent. In 2017, Li et al. announced that a phthalocyanine derivative can function as a photothermal substance when self-assembled and then be partially decomposed by proteins in vivo and act as a photodynamic substance (Fig. 1).[90] The system can function as a one-for-all system containing single components. Compared with the monomer, the absorption spectrum of the nanostructure (NanoPcTBs) was blue-shifted and expanded. In reference to Kasha's exciton theory, the H aggregate was formed by face-to-face stacking. This supramolecular assembly suppressed fluorescence emissions through enhanced ISC, which resulted in super-quenching of fluorescence emissions and high photothermal activity. When the NanoPcTBs were irradiated with a laser, the temperature increased by more than 33° compared with the results with pure water and generated a PA signal that had a high correlation with the photothermal effect. As a result, the NanoPcTBs achieved photothermal activity and PA imaging through supramolecular assembly, making them a material suitable for fluorescence imaging and PDT activation with an avidin trigger. The nanostructures actively and passively accumulated in the tumor, which was confirmed by fluorescence and PA imaging after an in vivo injection, and the photodynamic efficacy was good, inhibiting 40% of tumor growth after laser irradiation. This very promising tumor-targeting fusion therapy with its nanostructure formation method enables synergistic treatment by inducing photothermal effects from self-assembled supramolecular formations of photodynamic agents, and it minimizes side effects through switchable photoactivity.

In 2019, Song et al. developed organic photosensitizers that can initiate both PTT and PDT with a single wavelength of light (Fig. 2).[91] Their designed diiodo-distyryl-TEG-borondipyrromethene (TBDP) forms stable nanoparticles (TBDP NPs) in aqueous solutions and has photothermal and photodynamic efficacy. In their intracellular experiment, irradiation with 635 nm light generated both a single antioxidant

Fig. 1 Schematic illustration of the assembly and partial disassembly processes of NanoPcTBs. Reproduced with permission from ref. 90. Copyright 2017, American Chemical Society.

Fig. 2 Chemical structure of TBDP and schematic illustrations of the therapeutic process of TBDP NPs. Adapted with permission from ref. 91.

and heat, producing excellent phototoxicity and light stability. Excellent phototoxicity was also confirmed in *in vivo* antitumor experiments.

A two-dimensional covalent organic framework (COF) can control the orderly spatial arrangement of organic molecules.[92] In 2019, Wang *et al.* reported a strategy to provide simultaneous PDT and PTT using a porphyrin-based COF of nanoparticles (COF-366 NPs) (Fig. 3).[93] The ordered spatial arrangement of the

COF-366 NPs reduced the aggregation and quenching of porphyrin, which improved ROS generation over that with single molecules. It also improved NIR absorption, making it possible to implement PA imaging and induce PTT. The COF-366 NPs provided simultaneous PDT and PTT in tumor-bearing mice irradiated with a single-wavelength light source.

2.2 Co-assembly of PDT and PTT components

The simplest strategy for combining PDT and PTT would be the supramolecular assembly of photodynamic and photothermal agents. In a study by Yu *et al.*, porphyrin derivatives (Pp4N) for PDT and graphene nanoribbons (GNR-PEO2000) that exhibit PTT functionality were supra-molecularly assembled through electrostatic attraction and then used to treat bacterial infections (Fig. 4).[94] The negatively charged bacterial cell wall interacted strongly with the Pp4N, a cationic porphyrin functionalized with four ammonium groups, which effectively treated the bacterial infections. Transmission electron microscopy (TEM) confirmed that the Pp4N aggregate was adsorbed onto GNR-PEO2000. Because the fluorescence intensity of the Pp4N increased as the ratio of GNR-PEO2000 increased during supramolecular assembly, the adsorption of Pp4N nanoparticles onto the GNR surface reduced the degree of aggregation, thereby reducing the aggregation-induced quenching effect and allowing the PS to work even in an aqueous solution. In addition, this supramolecular assembly provided much improved photostability compared with commercially available PSs. The Pp4N/GNR-PEO2000 nanocomposite acts as an excellent dual-mode PS by performing both ROS production (in PDT) and temperature elevation (in PTT) when irradiated with light at 660 nm and 808 nm, respectively. The system achieved the impressive antimicrobial effect of completely killing Gram-positive, Gram-negative, and drug-resistant bacteria both *in vitro* and *in vivo*.

In 2018, Han *et al.* developed oxygen-independent PDT and PTT systems (Fig. 5).[95] Three-block copolymer PEG-*b*-PCL-*b*-PPEMA co-encapsulates cypate and singlet oxygen-donor
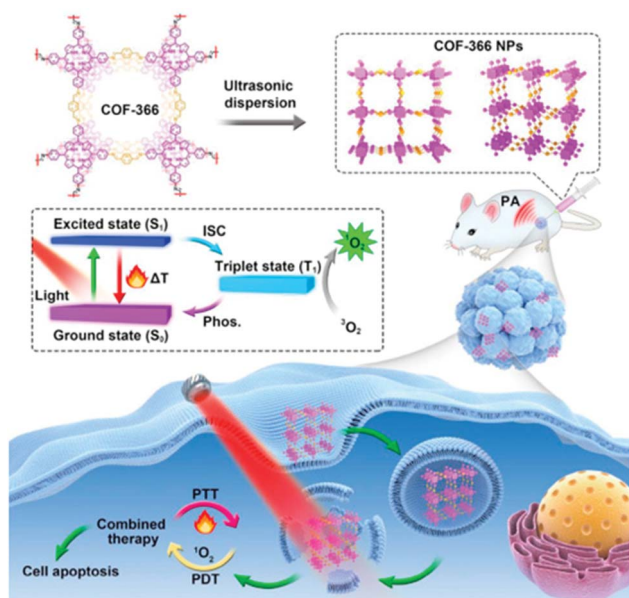

Fig. 3 Schematic illustration of the formation of COF–366 NPs and the phototherapy process. Reproduced with permission from ref. 93. Copyright 2019, Elsevier Ltd.

Fig. 4 Structure of Pp4N and GNR-PEO2000 and schematic illustrations of the double light–activated photodynamic and photothermal therapy for drug-resistant bacteria. Reproduced with permission from ref. 94. Copyright 2019, Wiley-VCH Verlag GmbH & Co. KGaA, Weinheim.
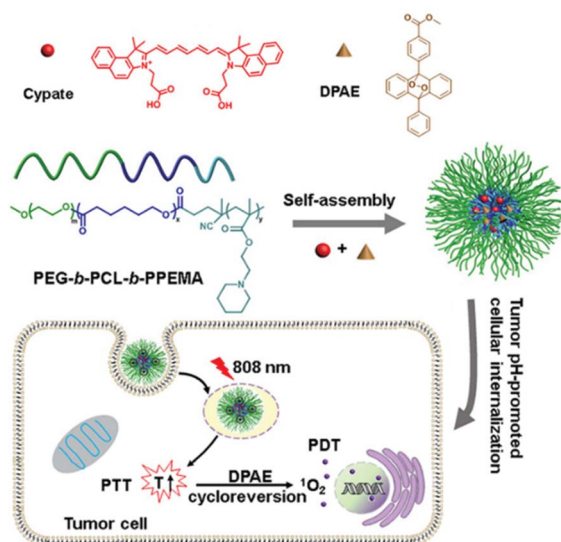
Fig. 5 Chemical structure of the C/O@N-Micelle and schematic illustration of its pH-responsive cellular uptake and oxygen-independent photothermal/photodynamic therapy. Reproduced with permission from ref. 95. Copyright 2018, Elsevier B.V.

diphenylanthracene endoperoxide (DPAE) *via* self-assembly to obtain a new synergistic nano-micelle system (C/O@N-Micelle). The micelles exhibited 2.1-fold improved internalization under tumor pH conditions compared with neutral conditions. Under 808 nm NIR irradiation, cypate can generate strong heat by the PTT process, which induces the thermal cycle regression of DPAE to produce singlet oxygen. The oxygen-independent photothermal-induced PDT and PTT combination effectively inhibited tumor growth without causing significant systemic toxicity.

Gong *et al.* reported a multifunctional polymeric nano-micelle system containing IR825, a NIR dye, and photosensitive Ce6.[96] They first made a Ce6-grafted amphiphilic polymer (C18PMH-PEG-Ce6) and then used it to encapsulate IR825 and create IR825@C18PMH-PEG-Ce6 nano-micelles containing both a PS and a photothermal agent (Fig. 6). Ce6 also acts as a chelating agent for Gd^{3+}, enabling magnetic resonance (MR) imaging. With their high NIR absorbance, these theranostic micelles can be used as contrast media for triple mode MR, fluorescence, and PA imaging. The synergistic antitumor effect of the combined PTT and PDT was confirmed in a tumor-bearing mouse model.

To combine PTT and PDT, Chen *et al.* developed nano PSs using AIE materials (Fig. 7).[97] The novel AIEgen MeO-TPE-indo (MTi) can selectively target the mitochondria and effectively generate ROS. The authors formed PMTi, a nanocomposite of MTi and polydopamine nanoparticles by π–π lamination and hydrogen bonding. Polydopamine has strong absorbance and a high photothermal energy conversion efficiency in the NIR region. The resulting PMTi nanoparticle inhibited the growth rate and volume of mouse tumors *in vivo* when it was activated, respectively, by white light and an NIR laser.

In 2020, Wang *et al.* reported a PDT-PTT supramolecular assembly with the ability to supply its own oxygen (Fig. 8).[98] The photothermal agent polydopamine, the photodynamic agent Ce6, and hemoglobin (Hb) formed supramolecular assemblies ([PHC]PP@HA NPs). The rapid oxidation that hindered Hb's functioning as an oxygen donor was prevented through supramolecular assembly with polydopamine.[99,100] In addition, as reported by a previous study,[101] the combination of NIR dye and polydopamine can improve photothermal efficiency. Therefore, the supramolecular assembly in this design helped to overcome the hypoxia of the tumor microenvironment and increase photothermal efficiency. Polydopamine, Hb, and Ce6 formed nanoparticles under the ideal ratio conditions, and then they were packaged in polymer micelles and surface-modified with hyaluronic acid. The benzoimine bond between the poly(ethylene glycol) (PEG) and poly(ethylenimine) constituting the
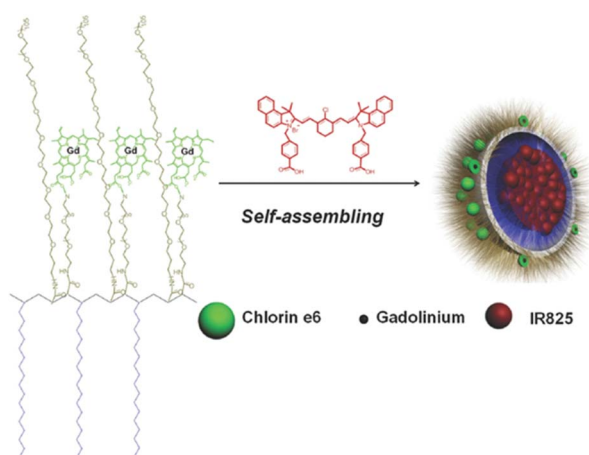

Fig. 6 A scheme showing the structure of the IR825@C18PMH-PEG-Ce6 nano-micelles. Reproduced with permission from ref. 96. Copyright 2014, WILEY-VCH Verlag GmbH & Co. KGaA, Weinheim.
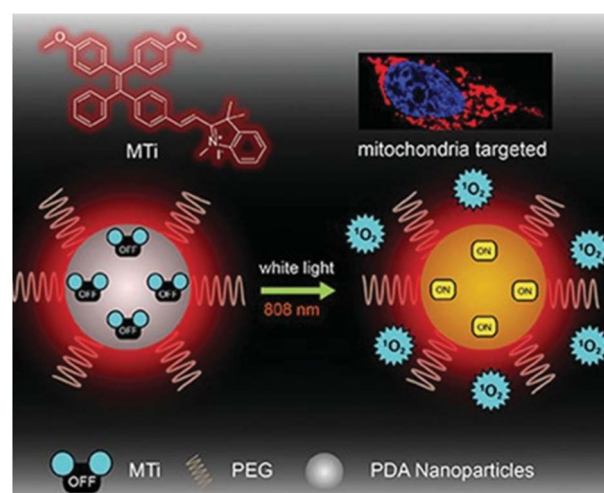

Fig. 7 Chemical structure of MTi and schematic illustration of the mitochondria-targeting white-light/NIR laser-activated photodynamic and photothermal therapy of the PMTi nanoparticle. Adapted with permission from ref. 97. Copyright 2019, WILEY-VCH Verlag GmbH & Co. KGaA, Weinheim.
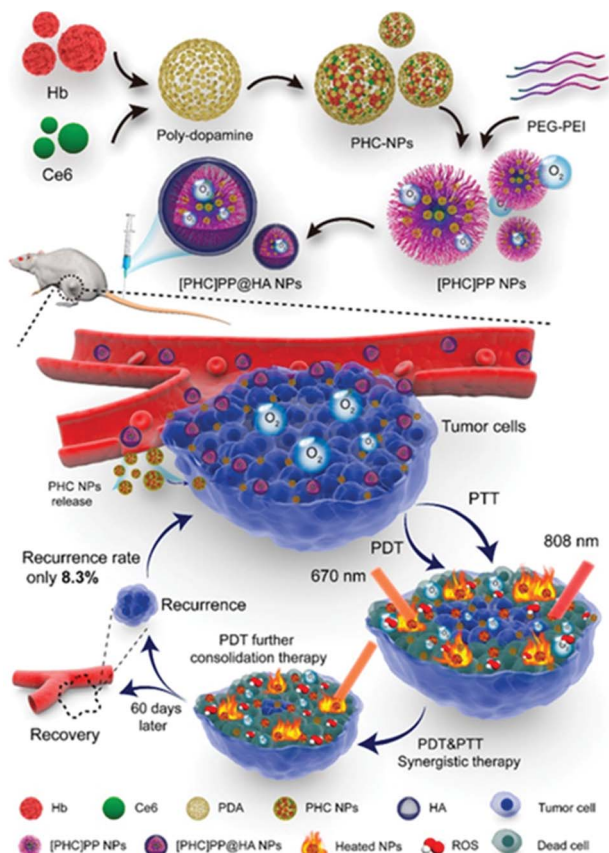
Fig. 8 Schematic illustration of the design and preparation of [PHC]PP@HA NPs for synergistic tumor PTT and PDT. Reproduced with permission from ref. 98. Copyright 2020, American Chemical Society. All rights reserved.

micelles is unstable under acidic conditions. Therefore, when the nanocapsule reached the tumor site, it degraded rapidly through the breaking of the benzoimine bond. Because the breakdown of nanosystems is faster in actively growing tumors and weaker in areas with weakly active tumor tissue, the efficiency of the treatment can be adjusted to match the tumor activity. This intelligent feedback treatment strategy can prevent damage to normal tissue. The [PHC]PP@HA NP showed strong absorption in the NIR region and achieved a temperature increase of 38.1 °C, much higher than that of free Ce6 and polydopamine, within 10 minutes of irradiation with an 808 nm laser. Laser irradiation at 670 nm followed by laser irradiation at 808 nm induced rapid ROS generation. *In vivo* experiments demonstrated that this nanosystem can accumulate tumor-selectively and that real-time fluorescence imaging is possible. When the antitumor effect of the PTT/PDT was measured *in vivo*, the tumor inhibition rate (TIR) was close to 100% within 30 days.

2.3 Other supramolecular structures

Two-dimensional nanomaterials have a variety of interesting properties. In 2014, Liu *et al.* reported physical adsorption of the photodynamic agent Ce6 on non-toxic PEGylated MoS_2 with
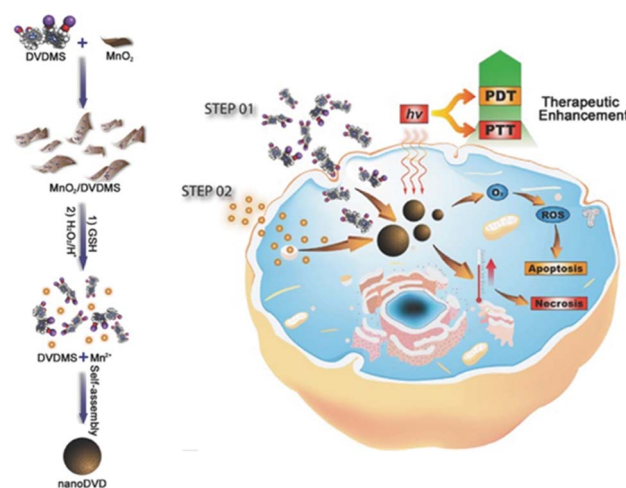

Fig. 9 Schematic illustration showing the fabrication and PDT and PTT process of MnO_2/DVDMS. Adapted with permission from ref. 103. Copyright 2017, John Wiley and Sons.

a very high surface area.[102] They used the powerful NIR absorbance of this nanomaterial to improve coupled PDT and PTT in both *in vitro* and *in vivo* animal experiments. Recently, Chu *et al.* deduced that Mn^{2+} can harmonize with the porphyrin ring and carboxylate radical of the sinoporphyrin sodium (DVDMS) molecule (Fig. 9).[103] Surprisingly, DVDMS formed nano-assemblies when it was simply dropped into a Mn^{2+} solution. The fluorescence of DVDMS mixed with Mn^{2+}, NanoDVD, was slightly quenched, but the efficiency of both PDT and PTT was increased. In the formation of supramolecules, the Mn^{2+} is thought to have strengthened the ISC and increased ROS production by increasing the population of the triplet state of DVDMS. The improved PTT effect was thought to result from stacking the porphyrin at a high density. As a result, the supramolecular binding of Mn^{2+} and DVDMS enabled the assembly of nanostructures that could simultaneously exhibit enhanced PDT and PTT activity. Next, the authors adsorbed DVDMS onto MnO_2 nanosheets because MnO_2 can be reduced to Mn^{2+} by intracellular glutathione (GSH), which also converts H_2O_2 into O_2. Using MCF-7 cells, they confirmed that the MnO_2/DVDMS downregulated the expression of hypoxia inducer 1α (HIF-1α), which was expected to improve the efficiency of PDT by alleviating hypoxia. The MnO_2 nanosheets improved the efficacy of phototherapy by supplying oxygen and releasing nanoDVDs, as well as by being a carrier for successful PDT. *In vivo*, the MnO_2/DVDMS provided fluorescence, MR, and PA imaging. The MR and PA signals disappeared within 24 hours, whereas the reduction of MnO_2 by GSH in the tumor environment and drug release increased the fluorescence signal. In addition, tumor-bearing mice injected with MnO_2/DVDMS showed a more marked reduction in tumor growth than mice receiving DVDMS and DVDMS combined with Mn^{2+}. This supramolecular engineering nanoplatform using coordination bonds achieved a synergistic combination of PTT and PDT along with multimodal imaging (fluorescence, MR, and PA imaging).

3. Supramolecular agents to combine PDT and chemotherapy

Chemotherapy (CHT) is the most commonly used traditional treatment modality in the field of oncology. However, CHT often requires multiple administrations, which can lead to drug resistance. In addition, therapeutic efficacy is limited by the ability of the drug to accumulate in the tumor.[104,105] PDT works locally to treat primary tumors, but it cannot treat metastatic cancer, and recurrence is often seen. Using PDT in combination with CHT is an interesting concept that could provide a more potent effect by treating tumor tissue that PDT cannot reach.[106] In addition, supramolecular nanocarriers made of PSs could selectively bring small-molecule anticancer drugs to tumor tissue. Although improved treatment results can be obtained with simple combination therapy, the combination of PDT and CHT shows a clear synergistic effect.

3.1 Co-assembly of PDT and CHT components

As discussed above, supramolecular assembly can suppress or improve the fluorescence and $^1O_2$ production of photodynamic materials, and it can also regulate activity through the mechanisms of its decomposition. The supramolecular assembly of a molecule that exhibits chemical drug activity and a PDT molecule is not only a simple method for combining PDT and CHT but can also be a strategy to modulate the activity of both therapeutics. A study by Li *et al.* introduced a supramolecular assembly of zinc(II)phthalocyanine with substituted anionic groups (PcS) and mitoxantrone (MA), a common anticancer drug (Fig. 10).[107] UV-Vis results showed a reduced and extended Q band compared to the monomer, which suggests that the supramolecular assemblies could exist as H aggregates according to Kasha's exciton theory. The super-quenched properties of the supramolecular assembly quenched fluorescence completely and singlet oxygen production by 96.7%. As shown above, the suppressed fluorescence emission and ISC indicate that PcS-MA could be used as a photothermal agent. The anticancer mechanism of MA begins with its insertion into DNA, and the binding constant of MA and DNA is similar to that of PcS. Therefore, this supramolecular assembly is selectively dissociated by nucleic acids and shows activatable $^1O_2$ generation. Compared with the PcS monomer, PcS-MA showed a higher fluorescence signal and lasted for a longer time in

tumor tissues. Even without laser irradiation, the antitumor effect of PcS-MA was better than that of MA alone, which means that the supramolecular assembly can increase the CHT effect through increased accumulation and long-term action. Partial degradation of PcS-MA caused by the limited nucleic acid concentration allowed the PcS-MA to exhibit a mild PTT effect that improved the PDT effect by increasing blood flow in the tumor and alleviating tumor hypoxia. The subsequently released chemotherapy agent, MA, destroyed tumor cells outside the PDT range, and the antitumor effect of the supramolecular assembly was much improved over that of the monotherapy formulation.

Cheng *et al.* self-assembled a photothermal agent, Ag$_2$S, and a PS, Ce6, into nanoclusters (Fig. 11).[108] In the nanocluster state, the fluorescence of Ce6 was quenched by 89.6% by the Ag$_2$S, and the singlet oxygen production capacity was quenched by 92.7%. Thus, in this cluster, Ag$_2$S controlled the photodynamic efficiency and fluorescence by acting as a switch in the supramolecular structure. The nanoclusters were wrapped in a polymer into which a targeting group was introduced with doxorubicin (DOX), an anticancer drug. This supramolecular assembly, ACD-FA, selectively accumulated in tumor cells and then released Ce6, restoring its ability to produce singlet oxygen. The DOX loaded onto the nanostructures was released much faster in the acidic tumor microenvironment than in normal tissue. *In vitro* experiments confirmed that this nanomaterial was delivered specifically to FA receptor-expressing tumor cells and that it released Ce6 after transduction. *In vivo* experiments confirmed that this nanostructure could be used to track tumors using real-time fluorescence and PA imaging, and they confirmed that Ag$_2$S, Ce6, and DOX were effectively released by means of PTT and the acidic tumor microenvironment. In tumor suppression experiments, the PDT effect of the Ce6 combined with the PTT effect of the Ag$_2$S to show better efficacy
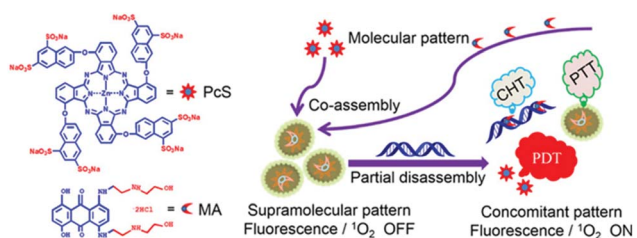
Fig. 10 Structures of octasulfonated phthalocyanine (PcS) and mitoxantrone (MA) and schematic illustration of the construction of the PcS–MA nanotheranostic agent. Adapted with permission from ref. 107. Copyright 2018, American Chemical Society.
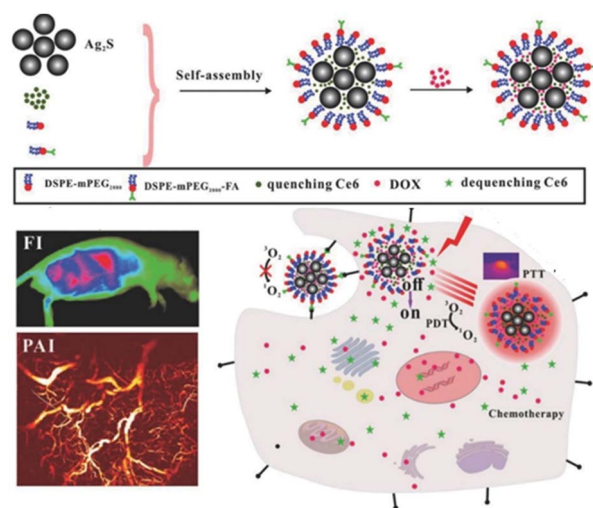

Fig. 11 Schematic illustration of the preparation of ACD–FA and the mechanism of its tumor targeting treatment. Reproduced with permission from ref. 108. Copyright 2018, WILEY–VCH Verlag GmbH & Co. KGaA, Weinheim.

than the single treatment, and the CHT effect of the released DOX inhibited tumor recurrence.

Most existing fluorophores have a disadvantageous quenching effect when aggregated, but AIE fluorogens (AIEgens) increase their fluorescence signal through high-concentration accumulation.[109–111] Therefore, AIEgens have an excellent signal-to-noise ratio, and they have been widely used in organelle imaging.[112–114] In addition, AIEgens can function as a therapeutic agent through CHT or PDT. Hu et al. reported that AIE-Mito-TPP molecules can selectively accumulate in the mitochondria of cancer cells, inducing apoptosis by reducing the mitochondrial membrane potential and inhibiting ATP synthesis.[115] Chen et al. developed supramolecular nanoparticles through self-assembly of AIE-Mito-TPP and AlPcSNa$_4$, a PS for PDT, to further improve cancer treatment efficiency (Fig. 12).[116] The fluorescence of the supramolecular nanoparticles was completely quenched by the fluorescence resonance energy transfer process between the two components and the self-quenching effect of π–π stacking. The AIE-Mito-TPP/AlPcSNa$_4$ NPs were absorbed by cancer cells through endocytosis and then decomposed by the lysosomal acidic environment and released into the cytoplasm. This process can be monitored in real time with dual-emission fluorescence tracking of the green emissions from the AIE-Mito-TPP and the red emissions from the AlPcSNa$_4$. The photodynamic effect of AlPcSNa$_4$ to destroy lysosomes combined with the ability of the AIE-Mito-TPP to efficiently destroy the mitochondrial function in vivo. This theranostic probe, capable of improved photodynamic efficacy and self-monitoring by double-luminescent fluorescence, has the potential benefits of developing supramolecular assembly therapeutics using AIE molecules.
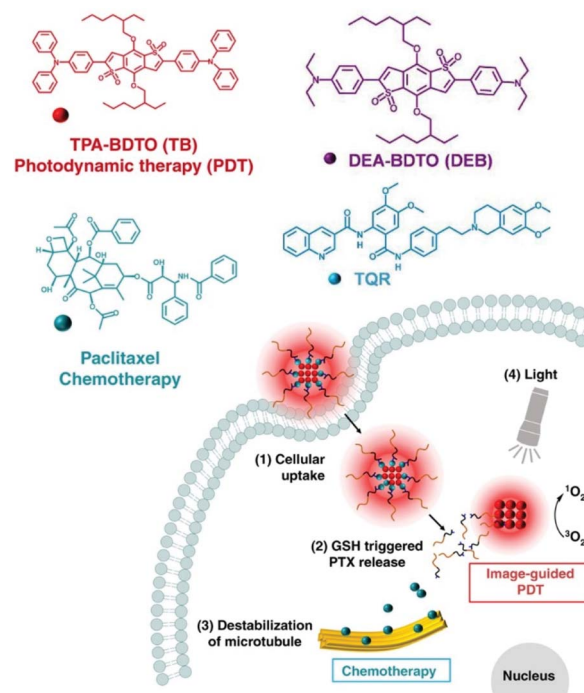
Fig. 13 Chemical structures of the components of TB@PMP and DEB/TQR@PMP and their internalization and therapy processes. Adapted with permission from ref. 117 and [118]. Copyright 2019, Elsevier Ltd.

Some researchers achieved a combination PDT and CHT therapy by loading AIEgens onto a self-assembled polymer prodrug. Yi et al. reported a nanoassembly that captured TB, an AIE-PS, with an anticancer prodrug containing paclitaxel (Fig. 13a).[117] High intracellular concentrations of GSH in tumor cells can release paclitaxel from polymeric prodrugs. In addition, decomposition of the polymer micelles led to the release of TB, with photodynamic effects. In vivo mouse experiments confirmed that the nanoassembly, TB@PMP, preferentially accumulated in the tumor area by EPR after intravenous injection. The results of antitumor experiments demonstrated that the nanoassemblies had synergistic tumor suppression effects compared with using PDT or CHT alone. Zhen et al. (Fig. 13b)[118] used a similar approach in 2019. They constructed DEB/TQR@PMP micelles by encapsulating the drug resistance inhibitor tariquidar (TQR) and NIR fluorophores (DEB-BDTO) within a polymeric prodrug (PMP). The DEB/TQR@PMP micelles also showed a remarkable synergistic antitumor effect by combining PDT and CHT.

Natural products that have traditionally been used as pharmaceuticals have good biodegradability and biocompatibility because they are derived from natural biological metabolisms. Various natural products are approved for use as anticancer drugs or are in clinical trials. Cheng et al. proposed a supramolecular system containing an anticancer drug (ergosterol) and a PS (Ce6) (Fig. 14).[119] A UV-Vis spectrum analysis of the Ergo-Ce6 NPs confirmed the presence of π–π stacking and hydrophobic interactions and showed that the Ce6 molecules existed mainly as monomers between stacked ergosterol molecules. In water, the Ergo-Ce6 NPs showed a fluorescence
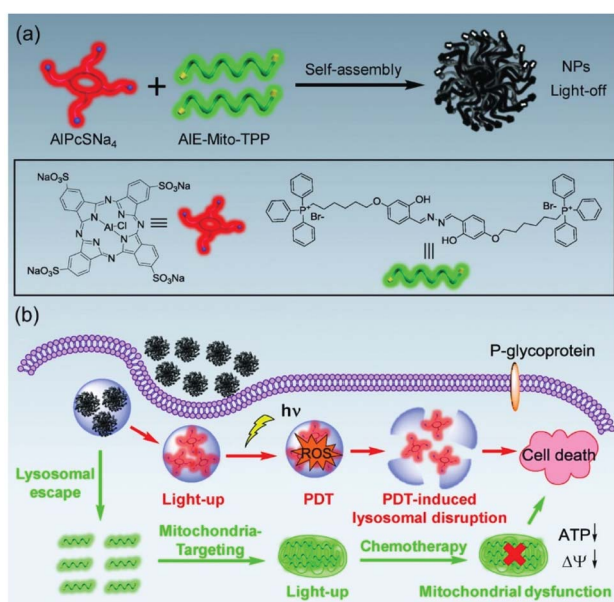

Fig. 12 (a) Scheme showing the preparation of AIE-Mito-TPP/AlPcSNa$_4$ NPs. (b) Schematic illustration of the synergistic chemo-photodynamic therapy functions of the AIE-Mito-TPP/AlPcSNa$_4$ NPs. Reproduced with permission from ref. 116. Copyright 2018, WILEY-VCH Verlag GmbH & Co. KGaA, Weinheim.
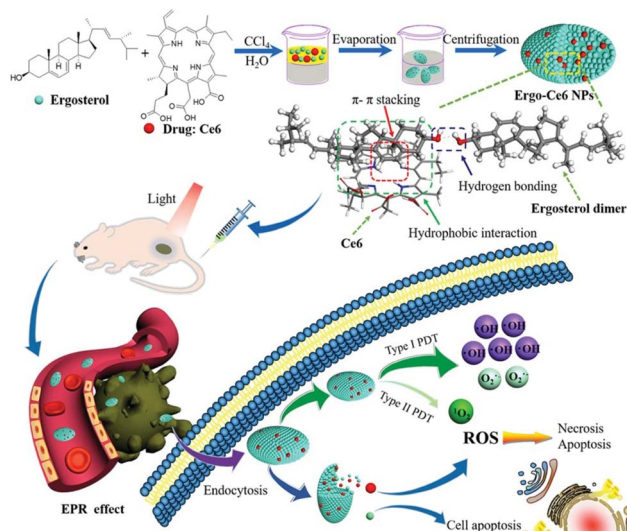
Fig. 14 Schematic illustration of the preparation of Ergo-Ce6 NPs and their efficiently combined antitumor therapy. Reproduced with permission from ref. 119. Copyright 2019, American Chemical Society.

Fig. 15 Chemical structure of the ICG@UA/PTX NPs and schematic illustration of the carrier-free small-molecule theranostic nanoplatform for chemo-phototherapy. Reproduced with permission from ref. 120. Copyright 2017, American Chemical Society.

quenching efficiency of about 93.7% compared to the monomer Ce6, but the heat generation process was not promoted. Suppressed fluorescence and vibrational relaxation can be expected to be transferred to the ISC process, leading to improved ROS generation. As expected, the Ergo-Ce6 NPs showed 1.4 times more ROS generation than Ce6. More specifically, the ·OH production of the Ergo-Ce6 NPs was 10 times higher than that of Ce6. Thus, the π–π interaction between Ce6 and the carrier ergosterol molecule caused by the encapsulation of Ce6 in the Ergo-Ce6 NPs mainly induced a type I photoreaction. In the hypoxic tumor microenvironment, type I reactions can exhibit higher efficiency than the oxygen-dependent type II reactions. The Ergo-Ce6 NPs demonstrated excellent tumor targeting ability and long-term blood circulation in *in vivo* fluorescence imaging. In an *in vivo* antitumor experiment, mice treated with Ergo-Ce6 NPs achieved 86.4% anticancer efficiency, which was much higher than that found in mice treated with Ergo NPs (51.0%) or Ce6 (59.5%) alone. The Ergo-Ce6 NPs, which were constructed using natural products without complex chemical modification, eliminated the aggregation problem of Ce6 and promoted the type I reaction. Thus, the supramolecular assembly with ergosterol provided synergistic anticancer effects while also providing biocompatibility and physical stability to ensure safe tumor treatment.

In 2017, Gao *et al.* developed a carrier-free nanosystem with self-assembly of the natural product ursolic acid (UA), the chemical drug paclitaxel (PTX), and photodynamic ICG based on electrostatic and π–π stacking interactions (Fig. 15).[120] UA induces apoptosis of cancer cells and prevents metastasis, but its low solubility hinders its clinical application. PTX is one of the most clinically used CHT drugs, but it also has low solubility. ICG is an FDA-approved NIR fluorescent probe that can be used in PTT and PDT. The three components self-assembled into a uniform size in an aqueous solution to form a stable

nanodrug delivery system, ICG@UA/PTX NPs. The UV spectra of the ICG@UA/PTX NPs showed a noticeable absorbance peak red shift and reduced fluorescence emissions due to the π–π conjugation effect. This supramolecular assembly improved the low-light stability of ICG and slowed the release rate of PTX. In addition, the NPs showed improved photodynamic and photothermal efficacy compared to free ICG. *In vivo* fluorescence imaging confirmed that the ICG@UA/PTX NPs showed excellent accumulation and long-term retention at the tumor site due to the EPR effect. In a tumor growth inhibition experiment in a tumor-bearing mouse model, when NIR laser-irradiated mice were injected with ICG@UA/PTX NPs, the TIR by tumor weight was 89.18 ± 1.19%, significantly higher than that when UA (14.22 ± 4.72%), PTX (25.75 ± 5.15%), and free ICG with NIR laser irradiation (66.50 ± 7.80%) were used separately.

In 2020, Zhang *et al.* went beyond the combination of PDT and CHT to investigate an improved synergistic combination using ultrasound (US) irradiation (Fig. 16).[121] They found that clinically used albumin-paclitaxel (HSA-PTX) nanoparticles could be combined with large amounts of DVDMS in an aqueous solution by simple mixing. The HSA-PTX-DVDMS nanoparticles (HPD) obtained in that way exhibited excellent stability and intratumoral accumulation after intravenous administration. Interestingly, the HPD showed an improved fluorescence signal and PDT efficacy compared with the aqueous DVDMS solution. Focusing on the fact that low-frequency US irradiation can promote drug release and cellular uptake,[122] 10–30 minutes of US irradiation was performed intracellularly on the HPD. This treatment promoted the intracellular absorption of HPD and improved its antitumor effect. HPD is a biocompatible, synergistic, nano-therapeutic agent consisting entirely of drugs already in clinical use.
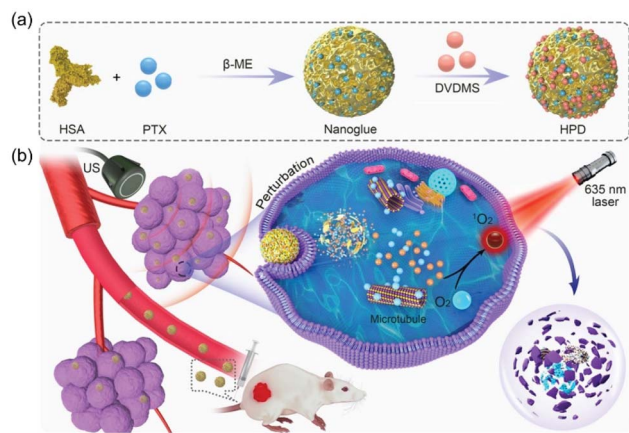
Fig. 16 Chemical structure of HSA–PTX–DVDMS (HPD) nanoparticles and schematic illustration of their combined PDT/CHT process enhanced by ultrasonic irradiation. Adapted with permission from ref. 121. Copyright 2020, American Chemical Society.

3.2 Supramolecular drug carrier containing a PS

Nanocarriers that mimic the structure of liposomes (hydrophilic core and hydrophobic bilayer) are widely used in the field of drug delivery. In 2011, Lovell *et al.* reported a liposome self-assembly structure composed of a phospholipid–porphyrin complex under the name 'porphysome'.[88] The porphyrin-implanted lipids in the nanovesicles were conjugated at a high density, resulting in fluorescence quenching and remarkable heat generation. This liposome system is a promising way of making nanomaterials for PDT and PTT. In 2011, Liang *et al.* introduced an excellent supramolecular nanosystem for synergistic PDT and CHT using previously reported porphyrin-transplanted lipids (PGL).[123] Hameed *et al.* used porphyrin-containing phospholipids to encapsulate DOX, a water-soluble CHT drug, as a multifunctional nanocarrier for fluorescent imaging-induced synergistic chemo-PDT (Fig. 17).[124] The interaction between DOX and PGL decreased the absorption of the Soret band of porphyrin and shifted the 4 nm wavelength of the maximum absorption field, but the fluorescence was not completely quenched. The system maintained its optical properties even after the DOX was encapsulated in the PGL NPs. As the DOX concentration increased, the fluorescence intensity of the PGL gradually decreased. This change demonstrates that resonance energy transfer from PGL to DOX occurs within the nanosystem. The interaction of PGL and DOX can

improve the circulation half-life by preventing explosive drug release during circulation. The PGL-DOX NPs prevented aggregation and provided a useful fluorescence signal while achieving very high porphyrin loading. Intracellular fluorescence imaging experiments confirmed that the PGL-DOX NPs were specifically delivered to lysosomes and that high cell delivery efficiency was achieved. The tumor inhibition efficiency of the PGL-DOX NPs *in vivo*, evaluated in a subcutaneous xenograft mouse model, was significantly higher than that found in the single-treatment group.

Ji *et al.* reported a nanosystem that improved the efficiency of PDT by using an AIE photodynamic effect (Fig. 18).[125] The constituents of the prodrug monomer were the RGD protein that binds $\alpha_v\beta_3$ to facilitate tumor-selective delivery, the anti-cancer drug camptothecin (CPT), and the PS ICy5. No spectral overlap or peak shift was observed in the CPT and ICy5 moieties after chemical conjugation, suggesting that no charge or energy transfer occurred between the two fluorophores. ICy5-CPT-RGD is amphiphilic and can easily self-assemble in water to form micelles, PTN, with hydrophilic surfaces and hydrophobic inner parts. In the examination of the $^1O_2$ generation efficiency of the PTN, using DPBF (1,3-diphenylisobenzofuran) as a probe, the $\Phi(^1O_2)$ of PTN was 26.2%, about 10 times stronger than the 2.7% of the single-molecule ICy5-CPT-RGD in DMSO. The enhanced photodynamic effect was attributed to enhanced ISC. When PTN generates singlet oxygen through PDT, the decomposition of ICy5 could be induced, and the nanoparticles might collapse. In cell experiments, the red fluorescence of ICy5 coincided with the green fluorescence of Lysotracker Green, confirming that PTN accumulated in lysosomes. The acidic conditions of lysosomes also allow hydrolysis of the ester bonds in the PTN, which can lead to CPT release. *In vivo* fluorescence images showed that a strong signal accumulated at the tumor

Fig. 17 Schematic illustration of the synthesis process for PGL-DOX NPs. Adapted with permission from ref. 124.
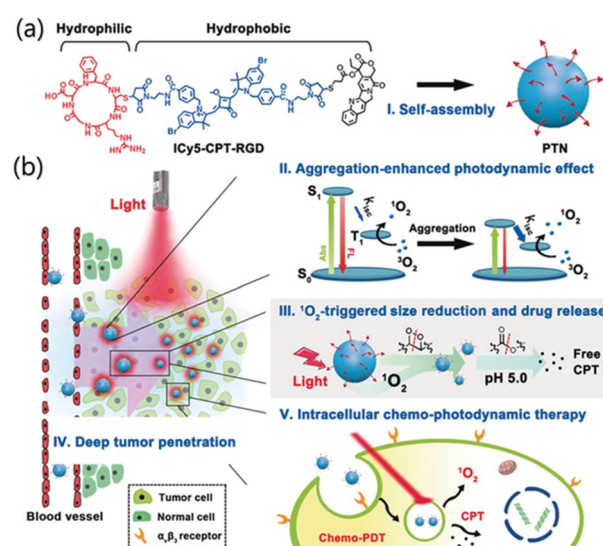

Fig. 18 (a) Chemical structure of ICy5-CPT-RGD formed as PTN. (b) Schematic illustration of the characteristics and delivery process of PTN. Reproduced with permission from ref. 125. Copyright 2018, Wiley-VCH Verlag GmbH & Co. KGaA, Weinheim.

Fig. 19 Schematic illustration of polymeric micelles for synergistic cancer chemotherapy. Adapted with permission from ref. 126. Copyright 2021, Elsevier B.V.

red shifted, from 673 nm to 820 nm, due to the π–π stacking interaction of the hydrophobic aromatic ring. The accumulation of this micelle, DIR, was trackable into the tumor site through fluorescence imaging. Antitumor experiments showed improved anti-tumor efficiency compared with each monotherapy.

3.3 Other supramolecular structures

The host–guest complexing strategy is one promising method to create supramolecular structures, allowing convenient control of the ratio between components. In 2015, Meng and colleagues reported a supramolecular system in which DOX was loaded into supramolecular vesicles based on host–guest interactions between water-soluble PA [5] and a BODIPY derivative (WP5⊃G) (Fig. 20a).[127] In 2018, a vesicle encapsulating the prodrug tirapazamine, which is activated in hypoxia, was reported (Fig. 20b).[128] These researchers used NIR-absorbing diketopyrrolopyrrole-based guest G as a photothermal agent and PS to construct multifunctional supramolecular vesicles based on the recognition of water-soluble pillars [5] arene (WP5) and G. In late 2018, Yang et al. built a multifunctional supramolecular system based on a host–guest complex between an ada-functionalized Ru(II) complex and β-CD (Fig. 20c).[129] Three-dimensional self-assembled nanoparticles of Fu/LD@RuCD were co-loaded with two drugs (5-fluorouracil and ronidamine) that act on different targets. Upon visible light irradiation, the Fu/LD@RuCD showed excellent PDT ability, and its anticancer efficacy was much better than that of the single treatment modality.

Lim et al. introduced a self-assembled supramolecular nanocarrier (PEG-Por-CD:oxliPt (IV)-ada) that can deliver PSs and prodrugs simultaneously (Fig. 21).[130] The adamantane-modified oxaliplatin prodrug (oxliPt(IV)-ada) and a β-cyclodextrin-binding porphyrin PS (PEG-Por-CD) were assembled via host–guest binding between the adamantane and β-cyclodextrin. After constructing the supramolecular system, the Soret band and Q bands of porphyrin showed a slight red shift, but the shape and intensity of the peak were almost maintained. In addition, when the supramolecular assembly was irradiated

site 24 hours after injection, indicating an excellent tumor targeting ability and long residence time. The tumor growth inhibition rate of the PTN combination therapy was 77.5%, which was higher than that of PDT (33.1%) or CPT (less than 20%) alone. This study was the first to reveal the aggregation-induced photodynamic effects of cyanine dyes.

Su et al. reported a polymer micelle loaded with hydrophobic DOX in a self-assembled star-shaped polymer PEG(-b-PCL-Ce6)-b-PBEMA (Fig. 19).[126] The Ce6 part of the polymer was used as a PS, and polycaprolactone served as a hydrophobic segment for micelle assembly. The third segment induced GSH depletion by releasing quinone methide by means of H₂O₂. Compared with free Ce6, the emission peak of the polymer micelles was strongly

Fig. 20 Schematic illustration of (a) WP5⊃G, (b) WP5/G, and (c) Fu/LD@RuCD. Adapted with permission from ref. 127–129. Copyright 2018, The Royal Society of Chemistry.
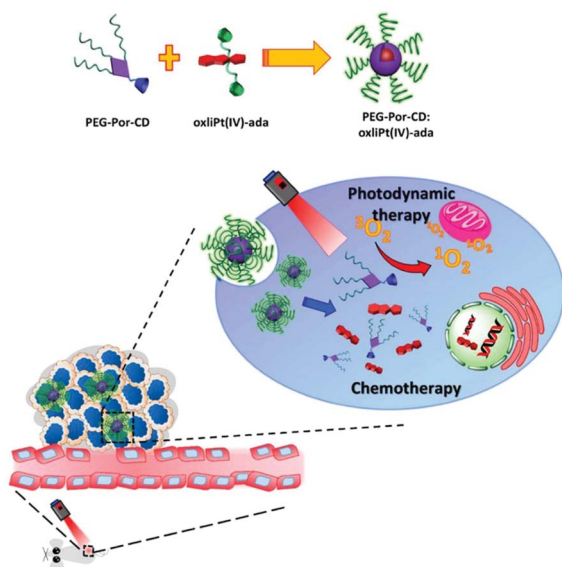
Fig. 21 Schematic illustration for the formation of PEG-Por-CD:ox-liPt(IV)-ada nanoparticles and their application in combined photodynamic therapy and chemotherapy for cancer. Adapted with permission from ref. 130. Copyright 2019, American Chemical Society.

with light at 630 nm, it showed slightly less efficient singlet oxygen generation than free porphyrin, likely due to self-quenching, but it was still sufficient for use in treatment. In *in vivo* antitumor experiments, the PEG-Por-CD:oxliPt(IV)-ada nanoparticles provided better tumor growth inhibition than PDT or CHT alone.

4. Supramolecular agents to combine PDT and immunotherapy

The 2018 Nobel Prize in Medicine or Physiology was awarded to James P. Allison of the University of Texas MD Anderson Cancer Center and Tasuku Honjo of the University of Kyoto for their contribution to cancer immunology.[131] Allison and Honjo's research in the field of cancer immunity has been a major breakthrough in cancer therapy. The simple summary of cancer immunotherapy is treating tumors by training antitumor immune cells to attack tumor cells that have been hiding to evade the immune system. Cancer treatment using an immune response can kill both primary and metastatic tumor cells and establish an immune memory that prevents tumor recurrence.

It should be noted that apoptosis induced by PDT results in the release of tumor-specific antigens, which enhances immunogenicity in the tumor microenvironment.[15] Because the effectiveness of phototherapy is localized and limited to the surface, tumor recurrence after treatment is common. Light therapy and immunotherapy are an ideal combination therapy that can simultaneously increase the immune response and prevent recurrence through the antigen release caused by PDT. Various PDT-immunotherapy combination strategies have been published to date, and this article summarizes those that used supramolecular assembly strategies.

4.1 Co-assembly of PDT and immunotherapy components

Immune checkpoint blocking therapy releases the brake on effector T cells using monoclonal antibodies that inhibit the signaling pathway of cell death 1 (PD-1) and its ligand (PD-L1).[132] Adaptive immune resistance is a self-protective mechanism that tumor cells use to defend against host immune responses.[133] PD-1 and PD-L1 are two important immune checkpoint molecules that are closely related to immune resistance.[134] Abnormally expressed in many cancers, including melanoma and breast cancer, PD-L1 promotes immune evasion and ultimately leads to tumor recurrence and metastasis.[135] PD-1-immunotherapy, which uses anti-PD-1 or anti-PD-L1 antibodies to block the PD-L1 signaling pathway, has shown antitumor effects in clinical studies.[136,137]

Xu *et al.* found that the PS Ce6 interacts with immunoglobulin G (IgG) antibodies with a higher affinity than it has for its endogenous carrier, human serum albumin (Fig. 22).[138] In the presence of polyvinylpyrrolidone (PVP), a pharmaceutical excipient, Ce6 and IgG spontaneously formed nanostructures about 30 nm in size called Chloringlobulin. This supramolecular assembly method improved the pharmacokinetics of Ce6. Nanosized PSs have traditionally been found to achieve tumor accumulation through the EPR effect, but Chloringlobulin used the "IgG hitchhiking" approach based on the high affinity of Ce6 for IgG. The Ce6 release profile confirmed that the IgG–Ce6 complex was stably present in serum, and after 2 hours, a significant amount of Ce6 was released and redistributed to the serum components. Unlike conventional nanostructures, Chloringlobulin showed increased tumor accumulation during the first few hours, and then the Ce6 was quickly eliminated by "hitchhiking" away from the IgG. Chloringlobulin was used in a glioma-bearing mouse model for Ce6-based intraoperative fluorescence image-guided resection, and it enabled more accurate tumor resection. When it was injected into colon cancer-bearing mice, metastatic lesions were found through fluorescence imaging. Chloringlobulin enabled fluorescence image-guided PDT, and it induced the highest survival rate, strong antitumor immunity, and improved memory T cells compared with the control group.

Fig. 22 Schematic illustration of a Chloringlobulin for photodynamic therapy combined with immune checkpoint blockade therapy. Reproduced with permission from ref. 138. Copyright 2019, American Chemical Society.

Fig. 23 Chemical structure of the acid-responsive POP micelleplex co-loaded with PPa and siRNA and a schematic illustration of photodynamic therapy combined with immunotherapy. Adapted with permission from ref. 139. Copyright 2016, American Chemical Society.

Wang *et al.* reported a multifunctional micelle nanoplatform (POP micelleplex) that can be activated in an acidic environment (Fig. 23).[139] POP micelleplex consists of a pH-responsive di-block copolymer and a covalently bonded pheophorbide A (PPa). These building blocks self-assemble into micelles under neutral conditions, and fluorescence is quenched by homogeneous fluorescence resonance energy transfer between the PPa molecules encapsulated inside the core. PD-L1-specific siRNA, the second component of the POP micelleplex, suppresses the immune tolerance of tumor cells regulated by the PD-L1 pathway. The third component, 1,2-epoxy tetradecane alkylated oligoethylene imine, is an amphiphilic polycation that causes the endosome escape of siRNA payloads. The POP micelleplex generated a fluorescent signal after entering the weakly acidified tumor microenvironment. PPa, which is delivered to tumor cells by the breakdown of the micelles, underwent PDT and stimulated antitumor immune responses. The combined effect of the PDT-induced antitumor immune response and the blockade of the PD-L1–PD-1 pathway effectively inhibited tumor growth and metastasis.

4.2 Supramolecular drug carriers containing PSs

PDT induces immunogenic cell death of tumor cells, accompanied by the release of damage-related molecular patterns (DAMPs).[140] However, it has been reported that cellular apoptosis induced by conventional cytoplasmic localized PDT (CP-PDT) is less immunogenic than plasma membrane localized PDT (PM-PDT) due to slower DAMP release.[141] Zhang *et al.*

achieved rapid DAMP release after PDT using the chimeric peptide PpIX-C_6-PEG$_8$-KKKKKKSKTKC-OMe (PCPK), which targets the plasma membrane (PM) in tumor cells (Fig. 24).[142] The PCPK formed a supramolecular micelle structure in an

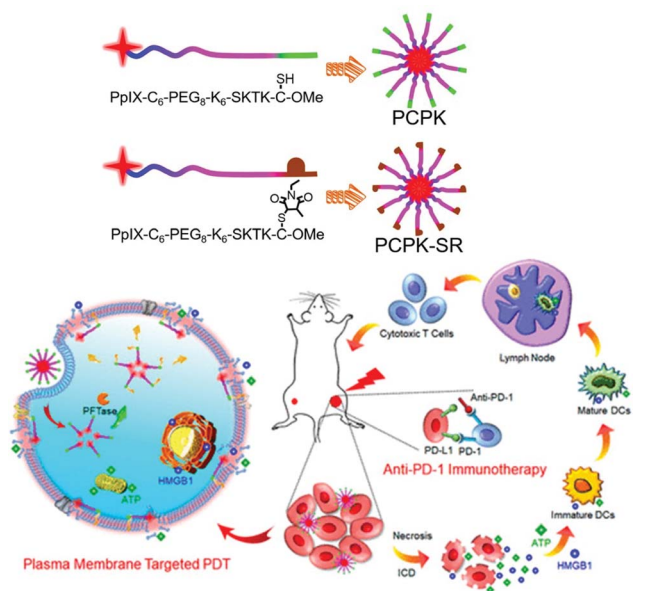

Fig. 24 Structures of PCPK, and PCPK–SR and schematic illustration of plasma membrane-targeted PDT (PM-PDT) combined with PD-1 checkpoint blockade therapy. Adapted with permission from ref. 142. Copyright 2019, American Chemical Society.

aqueous solution. The PM-targeted K-Ras-derived peptide KKKKKKSKTKC-OMe that is composed of PCPK can be delivered from the cytoplasm to the PM through subsequent enzymatic conversion by the protein farnesyl transferase.[143,144] PM-selective rupture of the PCPK micelles induced by PDT could make tumor cells potently immunogenic, resulting in a significantly improved antitumor immune response compared with conventional CP-PDT. Both *in vitro* and *in vivo* experiments confirmed that PM-PDT not only showed an improved antitumor effect compared with CP-PDT, but also induced a stronger immune response. The combination treatment of the chimeric peptide PCPK and the checkpoint blocker, anti-PD-1, achieved high antitumor effects in both primary and distant tumors.

He *et al.* developed self-assembled nanoscale coordination polymers (NCP)[145] to further develop their previously published NCP@pyrolipid, which has excellent anticancer efficacy (Fig. 25).[146] The NCP@pyrolipid combines the FDA-approved CHT drug oxaliplatin, CHT with a pyropheophorbide–lipid conjugate (pyrolipid), and an anti-PD-L1 checkpoint blockade for the treatment of colorectal cancer. Treatment with NCP@pyrolipid induced cancer cell apoptosis and activated an immune response through CHT and PDT. In a mouse model of colorectal cancer, NCP@pyrolipid inhibited primary tumor growth and enhanced the PD-L1 checkpoint blockade therapy to achieve excellent anticancer efficacy.
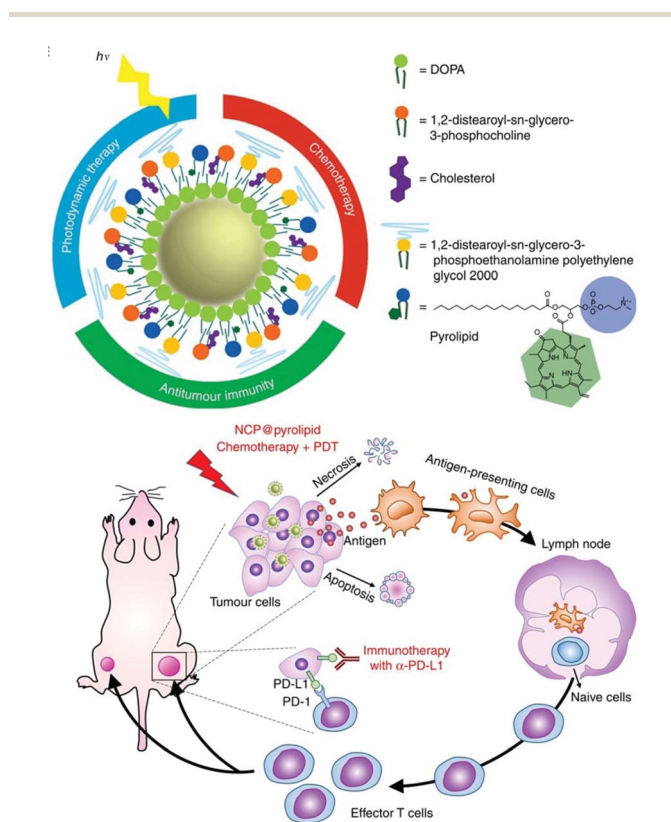
Indoleamine 2,3-dioxygenase (IDO), an enzyme overexpressed in tumor tissue, is an immune checkpoint that enhances the immunosuppression modulated by $CD4^+$ and causes the anergy and apoptosis of $CD8^+$ T cells.[147] Therefore, inhibiting IDO can strengthen the immune response to a tumor and prevent tumor recurrence. 1-Methyltryptophan (1MT) is a drug that inhibits IDO, but its use as a monotherapy has not shown satisfactory anticancer effects.[148] As mentioned above, the explosive release of tumor antigens by PDT can promote an immune response, so PDT might compensate for the deficiencies of 1MT immunotherapy. Song *et al.* combined the PS PpIX and the IDO inhibitor 1MT with Asp-Glu-Val-Asp, a caspase-3-sensitive peptide released from tumor cells (Fig. 26).[149] The chimeric peptide PpIX-1MT formed well-dispersed nanoparticles of about 50 nm in an aqueous solution. The formation of self-assembled nanoparticles, PpIX-1MT NPs, prevented the coagulation-induced quenching of PpIX so that high ROS generation could be maintained even in aqueous solutions. In *in vivo* distribution and tumor imaging experiments, distinct fluorescence was observed at the tumor site 2 hours after injection of the PpIX-1MT NPs. In the tumor growth inhibition experiment, the group irradiated with a laser after a PpIX-1MT NP injection showed maximal tumor growth inhibition compared with the other groups. It was also confirmed that lung metastases, in addition to primary tumors, were greatly suppressed by combination therapy with 1MT. The immunocytometry and immunofluorescence results also confirmed the improved immune response *in vivo*.

In 2019, an activatable PDT prodrug vesicle using a strategy similar to the IDO-mediated immune evasion was reported (Fig. 27).[150] NLG919, consisting of a PS and an IDO inhibitor linked by an enzyme-reactive PEG linker, maintained a stable nanostructure in the bloodstream, prevented drug leakage, and silenced the PDT effect to prevent phototoxicity in blood

Fig. 25 Schematic illustration of the structure of NCP@pyrolipid and the Induction of ICD by chemotherapy and PDT. Adapted with permission from ref. 146. Copyright 2016, Springer Nature.

Fig. 26 Chemical structure of the chimeric peptide PpIX–1MT and self-assembled PpIX–1MT NPs and schematic illustration of the light activated therapeutic process. Adapted with permission from ref. 149. Copyright 2018, American Chemical Society.

Fig. 27 Chemical structure of PDT prodrug vesicle and schematic illustration of photodynamic cancer immunotherapy by means of IDO-1 mediated immune invasion. Adapted with permission from ref. 150. Copyright 2020, American Chemical Society.

circulation. The prodrug vesicles accumulated and were activated specifically at the tumor site, and fluorescence imaging showed excellent antitumor efficacy and the induction of immune responses.

In addition, Liu *et al.* reported a strategy for loading an IDO inhibitor (NLG-8189) into self-assembled liposomes with phospholipid–porphyrin conjugates that respond to the high levels of GSH in the tumor microenvironment (Fig. 28).[151] The prepared IND@RAL suppressed fluorescence and photoactivity by means of a supramolecular assembly that can rapidly release PPa and an IDO inhibitor by cleaving a reduction-sensitive

Fig. 28 Chemical structure of IND@RAL and schematic illustration of GSH-induced PDT and immunotherapy. Reproduced with permission from ref. 151. Copyright 2019, American Chemical Society.

disulfide bond in a reducing tumor environment. Therefore, although the fluorescence signal and photoactivity maintain silence during blood circulation, the fluorescence signal (>100 times) and photoactivity (>100 times) are activated by the reducing microenvironment after tumor transfer. This also enables the selective release of IDO inhibitors in the tumor microenvironment. A flow cytometric analysis performed after laser irradiation demonstrated that IND@RAL-based PDT induced immunogenic cell death (ICD) responses in tumor cells, which could induce immune responses. *In vivo* fluorescence imaging in an orthotopic 4T1 tumor bearing mouse model confirmed that the IND@RAL signal successfully accumulated in the tumor, and its ability to inhibit primary and distant tumors and prevent lung metastases was demonstrated in antitumor experiments.

5. Conclusion and outlook

In summary, this review has summarized and discussed recent combinations of PDT with other therapeutic modalities that have been achieved using supramolecular approaches. The first point of the studies presented in this review is that they are supramolecular assembly nanomaterials. This review has described a variety of supramolecular nanosystems that improve treatment efficiency through the properties of supramolecular assembly. Supramolecular assembly can induce (i) controllable photophysical properties such as fluorescence, ROS production, and photothermal effects, (ii) activation in response to specific triggers, and (iii) the EPR effect to induce the selective accumulation of supramolecular nanosystems in tumors. The AIE and ACQ effects caused by supramolecular assembly create completely different photophysical properties from single molecules. As a result, useful changes can be achieved to make more effective treatments such as long wavelength absorption, PDT or PTT efficiency control, and fluorescence/PA imaging properties. The difference in photophysical properties between the supramolecular assembled nanostructure and the single component enables the formation of an activatable supramolecular therapeutic agent using the disassembly of supramolecular structure according to environmental changes. Supramolecular assembly can also be a method of imparting tumor selectivity. Nano-sized agents obtained by supramolecular assembly can be selectively delivered to tumors through the EPR effect, and higher tumor selectivity can be achieved by supramolecular assembly with the active targeting ligands.

The second point of the studies covered in this review is the combination of PDT with other therapies. Many nanostructured PS systems have already been developed to improve the transport and selectivity properties of PDT agents. However, no matter how improved the delivery efficiency, PDT is activated by light irradiation, so it is inherently difficult to use it to treat deep tissues or metastatic tumors untouched by light. Therefore, light therapy alone is usually unable to completely remove a tumor without recurrence, so combination therapy is required. In this review, we introduced novel studies that have achieved fusion with PTT, CHT, and Immunotherapy to

compensate for the shortcomings of the existing PDT. Several methods are being studied to integrate two or more treatments into one treatment system. Among them, supramolecular assembly is an efficient and simple method to fuse PDT with other therapies without covalent bonds. The design of supra-molecular PS systems, including the self-assembly of PSs, co-assembly with functional molecules, and loading of active agents into nano-delivery systems *via* supramolecular approaches, is a very promising strategy to induce new photo-physical properties and overcome the shortcomings of existing PDT paradigms.

The first combination therapy we have introduced is a dual therapy of photodynamic and photothermal agents. In Section 2, we introduced various PDT and PTT combination therapy systems, including therapeutic systems in which PTT properties are induced by supramolecular assembly. Unlike PDT, PTT kills tumor cells through local heat generation by laser irradiation. Therefore, PTT can complement the oxygen-dependent prop-erties of PDT because it does not use oxygen in tissues for cytotoxicity. Also important, self-assembly of some PSs can induce PTT properties by intermolecular interactions. However, because both PDT and PTT are local treatments activated by laser irradiation, the possibility of residual tumors cannot be excluded by using them in combination. In addition, the simple combination of a photodynamic agent and a photothermal agent can be cumbersome in clinical practice because it requires the use of two or more wavelength and intensity conditions.

Supramolecular PSs can function not only as therapeutic agents, but also as carriers. CHT is the most commonly used method of tumor treatment, but it has its disadvantages with its lack of tumor selectivity and several inherent side effects. Studies that have used this feature to address the shortcomings of CHT are discussed in Section 3. Nanosystems with the ablility to carry hydrophobic anticancer drugs with poor delivery effi-ciency to a tumor site improve the efficiency of CHT through passive or active delivery systems. The key to this combination is that because PSs are used as a nanocarrier to selectively deliver anticancer drugs, it is not simply a combination therapy, but a clear synergistic effect. The combination of phototherapy and CHT can reduce the likelihood of tumor recurrence after PDT. However, the laser irradiation time for PDT to achieve maximum efficiency needs further study to account for the timing of CHT drugs, and limitations such as insufficient loading efficiency remain.

Immune checkpoint blockade is a cancer treatment method that is receiving the most attention recently and is a new milestone in the field of cancer treatment. Despite its proven and impressive clinical efficacy, this treatment is still not applicable to most patients. Because the immunosuppressive tumor immune microenvironment (TIME) prevents the full expression of the anti-tumor efficacy of immune checkpoint suppression, this treatment is only applicable to a small number of patients. The release of immune substances through phototherapy can improve the low immune response rate, the biggest obstacle to clinical application of cancer immuno-therapy. Several studies discussed in Section 4 indicate that phototherapy induces an antitumor immune response that produces higher therapeutic efficiency than monotherapy and prevents recurrence. However, research on the immune response induced by PDT is still insufficient. Future research is needed on the cell-killing mechanism and immune response induced by PDT.

Considering the limitations of monotherapy, combination strategies hold promise for clinical applications. Supramolec-ular assembly is the most useful method for fusing several therapeutic substances. However, the clinical translation of supramolecular fusion systems is still very scarce and more research and development is needed. Studies on intermolecular interactions are still required to ensure that the photophysical changes induced by supramolecular assembly can be precisely controlled. An in-depth study of the self-assembly exercise process is essential. In addition, there is a need to increase the stability of supramolecular assemblies so that they respond only to the correct trigger and are stable against other stimuli. The investigation of the toxicity of each of the various components of the supramolecular assembly is also an important part. Although more research is needed, most supramolecular PSs are promising candidates for effective cancer treatment due to their biocompatibility and ease of manufacture.

Author contributions

N. Kwon contributed to literature curation and manuscript writing. H. Kim contributed to the editing of figures and manuscripts. J. Yoon and X. Li conceived and designed this review. All authors have read and approved the final manuscript.

Conflicts of interest

There are no conflicts to declare.

Acknowledgements

References

1 G. Feng, G.-Q. Zhang and D. Ding, *Chem. Soc. Rev.*, 2020, **49**, 8179–8234.
2 Á. Juarranz, P. Jaén, F. Sanz-Rodríguez, J. Cuevas and S. González, *Clin. Transl. Oncol.*, 2008, **10**, 148–154.
3 H. Ding, H. Yu, Y. Dong, R. Tian, G. Huang, D. A. Boothman, B. D. Sumer and J. Gao, *J. Controlled Release*, 2011, **156**, 276–280.
4 J. S. Dysart and M. S. Patterson, *Phys. Med. Biol.*, 2005, **50**, 2597.
5 E. Buytaert, M. Dewaele and P. Agostinis, *Biochim. Biophys. Acta, Rev. Cancer*, 2007, **1776**, 86–107.

6 T. Nakagawa, S. Shimizu, T. Watanabe, O. Yamaguchi, K. Otsu, H. Yamagata, H. Inohara, T. Kubo and Y. Tsujimoto, *Nature*, 2005, **434**, 652–658.

7 E. Buytaert, G. Callewaert, J. Vandenheede and P. Agostinis, *Autophagy*, 2006, **2**, 238–240.

8 P. Agostinis, K. Berg, K. A. Cengel, T. H. Foster, A. W. Girotti, S. O. Gollnick, S. M. Hahn, M. R. Hamblin, A. Juzeniene and D. Kessel, *Ca-Cancer J. Clin.*, 2011, **61**, 250–281.

9 V. Fingar, P. Kik, P. Haydon, P. Cerrito, M. Tseng, E. Abang and T. Wieman, *Br. J. Cancer*, 1999, **79**, 1702–1708.

10 V. H. Fingar, T. J. Wieman and P. S. Haydon, *Photochem. Photobiol.*, 1997, **66**, 513–517.

11 A. Ferrario, K. von Tiehl, S. Wong, M. Luna and C. J. Gomer, *Cancer Res.*, 2002, **62**, 3956–3961.

12 A. Ferrario, K. F. von Tiehl, N. Rucker, M. A. Schwarz, P. S. Gill and C. J. Gomer, *Cancer Res.*, 2000, **60**, 4066–4069.

13 D. Nowis, T. Stokłosa, M. Legat, T. Issat, M. Jakóbisiak and J. Gołąb, *Photodiagn. Photodyn. Ther.*, 2005, **2**, 283–298.

14 E. P. Chizenga and H. Abrahamse, *Pharmaceutics*, 2020, **12**, 632.

15 H. Hönigsmann, *Photochem. Photobiol. Sci.*, 2013, **12**, 16–21.

16 O. Raab, *Z. biol.*, 1900, **39**, 524–546.

17 H. v. Tappeiner and A. Jodlbauer, *Dtsch. Arch. Klin. Med.*, 1904, **80**, 427–487.

18 R. L. Lipson, E. J. Baldes and A. M. Olsen, *J. Thorac. Cardiovasc. Surg.*, 1961, **42**, 623–629.

19 I. Diamond, A. Mcdonagh, C. Wilson, S. Granelli, S. Nielsen and R. Jaenicke, *Lancet*, 1972, **300**, 1175–1177.

20 T. J. Dougherty, G. Grindey, R. Fiel, K. R. Weishaupt and D. Boyle, *J. Natl. Cancer Inst.*, 1975, **55**, 115–121.

21 T. J. Dougherty, J. E. Kaufman, A. Goldfarb, K. R. Weishaupt, D. Boyle and A. Mittleman, *Cancer Res.*, 1978, **38**, 2628–2635.

22 T. J. Dougherty, G. Lawrence, J. H. Kaufman, D. Boyle, K. R. Weishaupt and A. Goldfarb, *J. Natl. Cancer Inst.*, 1979, **62**, 231–237.

23 D. Kessel, *J. Clin. Med.*, 2019, **8**, 1581.

24 M. R. Hamblin, *Photochem. Photobiol.*, 2020, **96**, 506–516.

25 R. Baskaran, J. Lee and S.-G. Yang, *Biomater. Res.*, 2018, **22**, 1–8.

26 D. E. Dolmans, D. Fukumura and R. K. Jain, *Nat. Rev. Cancer*, 2003, **3**, 380–387.

27 W. Fan, P. Huang and X. Chen, *Chem. Soc. Rev.*, 2016, **45**, 6488–6519.

28 R. R. Allison and C. H. Sibata, *Photodiagn. Photodyn. Ther.*, 2010, **7**, 61–75.

29 R. Weijer, M. Broekgaarden, M. Kos, R. van Vught, E. A. Rauws, E. Breukink, T. M. van Gulik, G. Storm and M. Heger, *J. Photochem. Photobiol., C*, 2015, **23**, 103–131.

30 C. Shi, J. B. Wu and D. Pan, *J. Biomed. Opt.*, 2016, **21**, 050901.

31 E. Delaey, F. van Laar, D. De Vos, A. Kamuhabwa, P. Jacobs and P. de Witte, *J. Photochem. Photobiol., B*, 2000, **55**, 27–36.

32 Z. Sheng, D. Hu, M. Xue, M. He, P. Gong and L. Cai, *Nano-Micro Lett.*, 2013, **5**, 145–150.

33 P. Zhao, M. Zheng, C. Yue, Z. Luo, P. Gong, G. Gao, Z. Sheng, C. Zheng and L. Cai, *Biomaterials*, 2014, **35**, 6037–6046.

34 J. P. Tardivo, A. Del Giglio, C. S. De Oliveira, D. S. Gabrielli, H. C. Junqueira, D. B. Tada, D. Severino, R. de Fátima Turchiello and M. S. Baptista, *Photodiagn. Photodyn. Ther.*, 2005, **2**, 175–191.

35 E. Panzarini, V. Inguscio, G. M. Fimia and L. Dini, *PloS One*, 2014, **9**, e105778.

36 A. Kamkaew, S. H. Lim, H. B. Lee, L. V. Kiew, L. Y. Chung and K. Burgess, *Chem. Soc. Rev.*, 2013, **42**, 77–88.

37 V.-N. Nguyen, S. Qi, S. Kim, N. Kwon, G. Kim, Y. Yim, S. Park and J. Yoon, *J. Am. Chem. Soc.*, 2019, **141**, 16243–16248.

38 V. N. Nguyen, Y. Yim, S. Kim, B. Ryu, K. Swamy, G. Kim, N. Kwon, C. Y. Kim, S. Park and J. Yoon, *Angew. Chem., Int. Ed.*, 2020, **59**, 8957–8962.

39 S. Qi, N. Kwon, Y. Yim, V.-N. Nguyen and J. Yoon, *Chem. Sci.*, 2020, **11**, 6479–6484.

40 E. L. Cole, E. Arunkumar, S. Xiao, B. A. Smith and B. D. Smith, *Org. Biomol. Chem.*, 2012, **10**, 5769–5773.

41 M. R. Gill and J. A. Thomas, *Chem. Soc. Rev.*, 2012, **41**, 3179–3192.

42 Z. Hou, Y. Zhang, K. Deng, Y. Chen, X. Li, X. Deng, Z. Cheng, H. Lian, C. Li and J. Lin, *ACS Nano*, 2015, **9**, 2584–2599.

43 Z.-D. Qi, D.-W. Li, P. Jiang, F.-L. Jiang, Y.-S. Li, Y. Liu, W.-K. Wong and K.-W. Cheah, *J. Mater. Chem.*, 2011, **21**, 2455–2458.

44 H. Zhang, Y. Shan and L. Dong, *J. Biomed. Nanotechnol.*, 2014, **10**, 1450–1457.

45 Y. Cheng, A. C. Samia, J. D. Meyers, I. Panagopoulos, B. Fei and C. Burda, *J. Am. Chem. Soc.*, 2008, **130**, 10643–10647.

46 J. Wei, J. Li, D. Sun, Q. Li, J. Ma, X. Chen, X. Zhu and N. Zheng, *Adv. Funct. Mater.*, 2018, **28**, 1706310.

47 A. Jańczyk, E. Krakowska, G. Stochel and W. Macyk, *J. Am. Chem. Soc.*, 2006, **128**, 15574–15575.

48 D. Bechet, P. Couleaud, C. Frochot, M.-L. Viriot, F. Guillemin and M. Barberi-Heyob, *Trends Biotechnol.*, 2008, **26**, 612–621.

49 D. K. Chatterjee, L. S. Fong and Y. Zhang, *Adv. Drug Deliv. Rev.*, 2008, **60**, 1627–1637.

50 S. S. Lucky, K. C. Soo and Y. Zhang, *Chem. Rev.*, 2015, **115**, 1990–2042.

51 C.-K. Lim, J. Heo, S. Shin, K. Jeong, Y. H. Seo, W.-D. Jang, C. R. Park, S. Y. Park, S. Kim and I. C. Kwon, *Cancer Lett.*, 2013, **334**, 176–187.

52 H. Maeda, H. Nakamura and J. Fang, *Adv. Drug Deliv. Rev.*, 2013, **65**, 71–79.

53 V. Torchilin, *Adv. Drug Deliv. Rev.*, 2011, **63**, 131–135.

54 J. Fang, H. Nakamura and H. Maeda, *Adv. Drug Deliv. Rev.*, 2011, **63**, 136–151.

55 R. Bazak, M. Houri, S. El Achy, S. Kamel and T. J. Canc. Res. Clin. Oncol. Refaat, *J. Cancer Res. Clin. Oncol.*, 2015, **141**, 769–784.

56 S. D. Steichen, M. Caldorera-Moore and N. A. Peppas, *Eur. J. Pharm. Sci.*, 2013, **48**, 416–427.

57 M. J. Garland, C. M. Cassidy, D. Woolfson and R. F. Donnelly, *Future Med. Chem.*, 2009, **1**, 667–691.

58 Z. Huang, H. Xu, A. D. Meyers, A. I. Musani, L. Wang, R. Tagg, A. B. Barqawi and Y. K. Chen, *Technol. Canc. Res. Treat.*, 2008, **7**, 309–320.

59 M. Triesscheijn, P. Baas, J. H. Schellens and F. A. Stewart, *Oncologist*, 2006, **11**, 1034–1044.

60 Z. Xie, T. Fan, J. An, W. Choi, Y. Duo, Y. Ge, B. Zhang, G. Nie, N. Xie and T. Zheng, *Chem. Soc. Rev.*, 2020, **49**, 8065–8087.

61 X. Li, S. Lee and J. Yoon, *Chem. Soc. Rev.*, 2018, **47**, 1174–1188.

62 J. Zhou, L. Rao, G. Yu, T. R. Cook, X. Chen and F. Huang, *Chem. Soc. Rev.*, 2021, **50**, 2839–2891.

63 W. Feng, M. Jin, K. Yang, Y. Pei and Z. Pei, *Chem. Commun.*, 2018, **54**, 13626–13640.

64 M. J. Webber, E. A. Appel, E. Meijer and R. Langer, *Nat. Mater.*, 2016, **15**, 13–26.

65 R. Xing, T. Jiao, Y. Liu, K. Ma, Q. Zou, G. Ma and X. Yan, *Polymers*, 2016, **8**, 181.

66 Y. Liu, K. Ma, T. Jiao, R. Xing, G. Shen and X. Yan, *Sci. Rep.*, 2017, **7**, 42978.

67 L. Zhao, Y. Liu, R. Xing and X. Yan, *Angew. Chem., Int. Ed.*, 2020, **59**, 3793–3801.

68 X. Li, E. Y. Park, Y. Kang, N. Kwon, M. Yang, S. Lee, W. J. Kim, C. Kim and J. Yoon, *Angew. Chem., Int. Ed.*, 2020, **59**, 8630–8634.

69 X. Li, S. Kolemen, J. Yoon and E. U. Akkaya, *Adv. Funct. Mater.*, 2017, **27**, 1604053.

70 X. Li, B.-D. Zheng, X.-H. Peng, S.-Z. Li, J.-W. Ying, Y. Zhao, J.-D. Huang and J. Yoon, *Coord. Chem. Rev.*, 2019, **379**, 147–160.

71 Z. Guo, Y. Zou, H. He, J. Rao, S. Ji, X. Cui, H. Ke, Y. Deng, H. Yang and C. Chen, *Adv. Mater.*, 2016, **28**, 10155–10164.

72 Y. Yuan, C. J. Zhang, R. T. Kwok, S. Xu, R. Zhang, J. Wu, B. Z. Tang and B. Liu, *Adv. Funct. Mater.*, 2015, **25**, 6586–6595.

73 W. Wu, D. Mao, F. Hu, S. Xu, C. Chen, C. J. Zhang, X. Cheng, Y. Yuan, D. Ding and D. Kong, *Adv. Mater.*, 2017, **29**, 1700548.

74 B. Gu, W. Wu, G. Xu, G. Feng, F. Yin, P. H. J. Chong, J. Qu, K. T. Yong and B. Liu, *Adv. Mater.*, 2017, **29**, 1701076.

75 S. Liu, X. Zhou, H. Zhang, H. Ou, J. W. Lam, Y. Liu, L. Shi, D. Ding and B. Z. Tang, *J. Am. Chem. Soc.*, 2019, **141**, 5359–5368.

76 F. Würthner, T. E. Kaiser and C. R. Saha-Möller, *Angew. Chem., Int. Ed.*, 2011, **50**, 3376–3410.

77 H. He, S. Ji, Y. He, A. Zhu, Y. Zou, Y. Deng, H. Ke, H. Yang, Y. Zhao and Z. Guo, *Adv. Mater.*, 2017, **29**, 1606690.

78 M. H. Cheng, K. M. Harmatys, D. M. Charron, J. Chen and G. Zheng, *Angew. Chem., Int. Ed.*, 2019, **58**, 13394–13399.

79 D. R. Boraste, G. Chakraborty, A. K. Ray, G. S. Shankarling and H. Pal, *J. Photochem. Photobiol., A*, 2018, **358**, 26–37.

80 M. Mitsui, K. Higashi, R. Takahashi, Y. Hirumi and K. Kobayashi, *Photochem. Photobiol. Sci.*, 2014, **13**, 1130–1136.

81 M.-F. Tsai, S.-H. G. Chang, F.-Y. Cheng, V. Shanmugam, Y.-S. Cheng, C.-H. Su and C.-S. Yeh, *ACS Nano*, 2013, **7**, 5330–5342.

82 E. A. Hussein, M. M. Zagho, G. K. Nasrallah and A. A. Elzatahry, *Int. J. Nanomed.*, 2018, **13**, 2897.

83 M. Zhou, J. Li, S. Liang, A. K. Sood, D. Liang and C. Li, *ACS Nano*, 2015, **9**, 7085–7096.

84 X. Song, Q. Chen and Z. Liu, *Nano Res.*, 2015, **8**, 340–354.

85 J. Wang, G. Zhu, M. You, E. Song, M. I. Shukoor, K. Zhang, M. B. Altman, Y. Chen, Z. Zhu and C. Z. Huang, *ACS Nano*, 2012, **6**, 5070–5077.

86 B. Liu, C. Li, B. Xing, P. Yang and J. Lin, *J. Mater. Chem. B*, 2016, **4**, 4884–4894.

87 L. Zhao, Y. Liu, R. Chang, R. Xing and X. Yan, *Adv. Funct. Mater.*, 2019, **29**, 1806877.

88 J. F. Lovell, C. S. Jin, E. Huynh, H. Jin, C. Kim, J. L. Rubinstein, W. C. Chan, W. Cao, L. V. Wang and G. Zheng, *Nat. Mater.*, 2011, **10**, 324–332.

89 Q. Zou, M. Abbas, L. Zhao, S. Li, G. Shen and X. Yan, *J. Am. Chem. Soc.*, 2017, **139**, 1921–1927.

90 X. Li, C.-y. Kim, S. Lee, D. Lee, H.-M. Chung, G. Kim, S.-H. Heo, C. Kim, K.-S. Hong and J. Yoon, *J. Am. Chem. Soc.*, 2017, **139**, 10880–10886.

91 N. Song, L. Fu, Y. Liu, Y. Li, L. Chen, X. Wang, S. Liu and Z. Xie, *Dyes Pigm.*, 2019, **162**, 295–302.

92 Q. Fang, J. Wang, S. Gu, R. B. Kaspar, Z. Zhuang, J. Zheng, H. Guo, S. Qiu and Y. Yan, *J. Am. Chem. Soc.*, 2015, **137**, 8352–8355.

93 D. Wang, Z. Zhang, L. Lin, F. Liu, Y. Wang, Z. Guo, Y. Li, H. Tian and X. Chen, *Biomaterials*, 2019, **223**, 119459.

94 Z. H. Yu, X. Li, F. Xu, X. L. Hu, J. Yan, N. Kwon, G. R. Chen, T. Tang, X. Dong and Y. Mai, *Angew. Chem., Int. Ed.*, 2020, **59**, 3658–3664.

95 Y. Han, Z. Chen, H. Zhao, Z. Zha, W. Ke, Y. Wang and Z. Ge, *J. Controlled Release*, 2018, **284**, 15–25.

96 H. Gong, Z. Dong, Y. Liu, S. Yin, L. Cheng, W. Xi, J. Xiang, K. Liu, Y. Li and Z. Liu, *Adv. Funct. Mater.*, 2014, **24**, 6492–6502.

97 Y. Chen, W. Ai, X. Guo, Y. Li, Y. Ma, L. Chen, H. Zhang, T. Wang, X. Zhang and Z. Wang, *Small*, 2019, **15**, 1902352.

98 Y. Wang, S. Luo, Y. Wu, P. Tang, J. Liu, Z. Liu, S. Shen, H. Ren and D. Wu, *ACS Nano*, 2020, **14**, 17046–17062.

99 Q. Wang, R. Zhang, M. Lu, G. You, Y. Wang, G. Chen, C. Zhao, Z. Wang, X. Song and Y. Wu, *Biomacromolecules*, 2017, **18**, 1333–1341.

100 W. L. Liu, T. Liu, M. Z. Zou, W. Y. Yu, C. X. Li, Z. Y. He, M. K. Zhang, M. D. Liu, Z. H. Li and J. Feng, *Adv. Mater.*, 2018, **30**, 1802006.

101 H. Zhu, D. Qin, Y. Wu, B. Jing, J. Liu, D. Hazlewood, H. Zhang, Y. Feng, X. Yang and M. Wan, *ACS Appl. Mater. Interfaces*, 2018, **10**, 29251–29259.

102 T. Liu, C. Wang, W. Cui, H. Gong, C. Liang, X. Shi, Z. Li, B. Sun and Z. Liu, *Nanoscale*, 2014, **6**, 11219–11225.

103 C. Chu, H. Lin, H. Liu, X. Wang, J. Wang, P. Zhang, H. Gao, C. Huang, Y. Zeng and Y. Tan, *Adv. Mater.*, 2017, **29**, 1605928.

104 A. I. Minchinton and I. F. Tannock, *Nat. Rev. Cancer*, 2006, **6**, 583–592.

105 I. F. Tannock, C. M. Lee, J. K. Tunggal, D. S. Cowan and M. J. Egorin, *Clin. Cancer Res.*, 2002, **8**, 878–884.

106 D. Luo, K. A. Carter, D. Miranda and J. F. Lovell, *Adv. Sci.*, 2017, **4**, 1600106.

107 X. Li, S. Yu, D. Lee, G. Kim, B. Lee, Y. Cho, B.-Y. Zheng, M.-R. Ke, J.-D. Huang and K. T. Nam, *ACS Nano*, 2018, **12**, 681–688.

108 K. Cheng, X. Q. Yang, X. S. Zhang, J. Chen, J. An, Y. Y. Song, C. Li, Y. Xuan, R. Y. Zhang and C. H. Yang, *Adv. Funct. Mater.*, 2018, **28**, 1803118.

109 J. Qian and B. Z. Tang, *Chem*, 2017, **3**, 56–91.

110 J. Liang, G. Feng, R. T. K. Kwok, D. Ding, B. Tang and B. Liu, *Sci. China Chem.*, 2016, **59**, 53–61.

111 B. Liu, A. Pucci and T. Baumgartner, *Mater. Chem. Front.*, 2017, **1**, 1689–1690.

112 J. Mei, N. L. Leung, R. T. Kwok, J. W. Lam and B. Z. Tang, *Chem. Rev.*, 2015, **115**, 11718–11940.

113 G. Feng, W. Qin, Q. Hu, B. Z. Tang and B. Liu, *Adv. Healthcare Mater.*, 2015, **4**, 2667–2676.

114 C. Y. Yu, H. Xu, S. Ji, R. T. Kwok, J. W. Lam, X. Li, S. Krishnan, D. Ding and B. Z. Tang, *Adv. Mater.*, 2017, **29**, 1606167.

115 Q. Hu, M. Gao, G. Feng and B. Liu, *Angew. Chem., Int. Ed.*, 2014, **53**, 14225–14229.

116 X. Chen, Y. Li, S. Li, M. Gao, L. Ren and B. Z. Tang, *Adv. Funct. Mater.*, 2018, **28**, 1804362.

117 X. Yi, J. Dai, Y. Han, M. Xu, X. Zhang, S. Zhen, Z. Zhao, X. Lou and F. Xia, *Commun. Biol.*, 2018, **1**, 1–13.

118 S. Zhen, X. Yi, Z. Zhao, X. Lou, F. Xia and B. Z. Tang, *Biomaterials*, 2019, **218**, 119330.

119 J. Cheng, H. Zhao, L. Yao, Y. Li, B. Qi, J. Wang and X. Yang, *ACS Appl. Mater. Interfaces*, 2019, **11**, 29498–29511.

120 Y. Guo, K. Jiang, Z. Shen, G. Zheng, L. Fan, R. Zhao and J. Shao, *ACS Appl. Mater. Interfaces*, 2017, **9**, 43508–43519.

121 Y. Zhang, Y. Wan, Y. Chen, N. T. Blum, J. Lin and P. Huang, *ACS Nano*, 2020, **14**, 5560–5569.

122 A. K. Wood and C. M. Sehgal, *Ultrasound Med. Biol.*, 2015, **41**, 905–928.

123 X. Liang, X. Li, X. Yue and Z. Dai, *Angew. Chem., Int. Ed.*, 2011, **50**, 11622–11627.

124 S. Hameed, P. Bhattarai, X. Liang, N. Zhang, Y. Xu, M. Chen and Z. Dai, *Theranostics*, 2018, **8**, 5501.

125 C. Ji, Q. Gao, X. Dong, W. Yin, Z. Gu, Z. Gan, Y. Zhao and M. Yin, *Angew. Chem., Int. Ed.*, 2018, **57**, 11384–11388.

126 T. Su, F. Cheng, Y. Pu, J. Cao, S. Lin, G. Zhu and B. He, *Chem. Eng. J.*, 2021, 128561.

127 L.-B. Meng, W. Zhang, D. Li, Y. Li, X.-Y. Hu, L. Wang and G. Li, *Chem. Commun.*, 2015, **51**, 14381–14384.

128 Q. Wang, L. Tian, J. Xu, B. Xia, J. Li, F. Lu, X. Lu, W. Wang, W. Huang and Q. Fan, *Chem. Commun.*, 2018, **54**, 10328–10331.

129 G.-G. Yang, L. Hao, Q. Cao, H. Zhang, J. Yang, L.-N. Ji and Z.-W. Mao, *ACS Appl. Mater. Interfaces*, 2018, **10**, 28301–28313.

130 W. Q. Lim, G. Yang, S. Z. F. Phua, H. Chen and Y. Zhao, *ACS Appl. Mater. Interfaces*, 2019, **11**, 16391–16401.

131 Z. S. Guo, *BMC Cancer*, 2018, **18**, 1086.

132 S. L. Topalian, C. G. Drake and D. M. Pardoll, *Cancer Cell*, 2015, **27**, 450–461.

133 D. Hanahan and R. A. Weinberg, *Cell*, 2000, **100**, 57–70.

134 A. Dömling and T. A. Holak, *Angew. Chem., Int. Ed.*, 2014, **53**, 2286–2288.

135 D. M. Pardoll, *Nat. Rev. Cancer*, 2012, **12**, 252–264.

136 C. Wang, Y. Ye, G. M. Hochu, H. Sadeghifar and Z. Gu, *Nano Lett.*, 2016, **16**, 2334–2340.

137 H. N. Chang, B. Y. Liu, Y. K. Qi, Y. Zhou, Y. P. Chen, K. M. Pan, W. W. Li, X. M. Zhou, W. W. Ma and C. Y. Fu, *Angew. Chem., Int. Ed.*, 2015, **54**, 11760–11764.

138 J. Xu, S. Yu, X. Wang, Y. Qian, W. Wu, S. Zhang, B. Zheng, G. Wei, S. Gao and Z. Cao, *ACS Nano*, 2019, **13**, 10242–10260.

139 D. Wang, T. Wang, J. Liu, H. Yu, S. Jiao, B. Feng, F. Zhou, Y. Fu, Q. Yin and P. Zhang, *Nano Lett.*, 2016, **16**, 5503–5513.

140 D. V. Krysko, A. D. Garg, A. Kaczmarek, O. Krysko, P. Agostinis and P. Vandenabeele, *Nat. Rev. Cancer*, 2012, **12**, 860–875.

141 D. R. Green, T. Ferguson, L. Zitvogel and G. Kroemer, *Nat. Rev. Immunol.*, 2009, **9**, 353–363.

142 C. Zhang, F. Gao, W. Wu, W.-X. Qiu, L. Zhang, R. Li, Z.-N. Zhuang, W. Yu, H. Cheng and X.-Z. Zhang, *ACS Nano*, 2019, **13**, 11249–11262.

143 K. Weise, S. Kapoor, C. Denter, J. R. Nikolaus, N. Opitz, S. Koch, G. Triola, A. Herrmann, H. Waldmann and R. Winter, *J. Am. Chem. Soc.*, 2011, **133**, 880–887.

144 I. M. Ahearn, K. Haigis, D. Bar-Sagi and M. R. Philips, *Nat. Rev. Mol. Cell Biol.*, 2012, **13**, 39–51.

145 D. Liu, C. Poon, K. Lu, C. He and W. Lin, *Nat. Commun.*, 2014, **5**, 1–11.

146 C. He, X. Duan, N. Guo, C. Chan, C. Poon, R. R. Weichselbaum and W. Lin, *Nat. Commun.*, 2016, **7**, 1–12.

147 S. Löb, A. Königsrainer, H.-G. Rammensee, G. Opelz and P. Terness, *Nat. Rev. Cancer*, 2009, **9**, 445–452.

148 D. H. Munn and A. L. Mellor, *J. Clin. Invest.*, 2007, **117**, 1147–1154.

149 W. Song, J. Kuang, C.-X. Li, M. Zhang, D. Zheng, X. Zeng, C. Liu and X.-Z. Zhang, *ACS Nano*, 2018, **12**, 1978–1989.

150 A. Gao, B. Chen, J. Gao, F. Zhou, M. Saeed, B. Hou, Y. Li and H. Yu, *Nano Lett.*, 2019, **20**, 353–362.

151 D. Liu, B. Chen, Y. Mo, Z. Wang, T. Qi, Q. Zhang and Y. Wang, *Nano Lett.*, 2019, **19**, 6964–6976.